

# Leveraging Hamiltonian Simulation Techniques to Compile Operations on Bosonic Devices

Christopher Kang<sup>\*1, 2, 3</sup>, Micheline B. Soley<sup>\*4,5,6,7</sup>, Ella Crane<sup>8</sup>, S. M. Girvin<sup>6</sup>, and Nathan Wiebe<sup>2, 9, 10</sup>

<sup>1</sup>School of Computer Science, University of Washington, Seattle, WA 98195 USA

<sup>2</sup>Pacific Northwest National Laboratory, Richland, WA 99354 USA

<sup>3</sup>Department of Computer Science, University of Chicago, Chicago, IL 60637 USA

<sup>4</sup>Department of Chemistry, University of Wisconsin-Madison, 1101 University Ave.,  
Madison, WI 53706 USA

<sup>5</sup>Department of Physics, University of Wisconsin-Madison, 1150 University Ave., Madison,  
WI 53706 USA

<sup>6</sup>Yale Quantum Institute, 17 Hillhouse Ave., PO Box 208 334, New Haven, CT 06520-8263  
USA

<sup>7</sup>Department of Chemistry, Yale University, 225 Prospect St., New Haven, CT 06511 USA

<sup>8</sup>Joint Quantum Institute & Joint Center for Quantum Information and Computer Science,  
NIST/University of Maryland, College Park, Maryland, 20742 USA

<sup>9</sup>Department of Computer Science, University of Toronto, ON M5G 1Z7 Canada

<sup>10</sup>Canadian Institute For Advanced Research / Institut Canadien de Recherches Avancées,  
ON M5G 1Z7 Canada

## Abstract

Circuit QED enables the combined use of qubits and oscillator modes. Despite a variety of available gate sets, many hybrid qubit-boson (i.e., oscillator) operations are realizable only through optimal control theory (OCT) which is oftentimes intractable and uninterpretable. We introduce an analytic approach with rigorously proven error bounds for realizing specific classes of operations via two matrix product formulas commonly used in Hamiltonian simulation, the Lie–Trotter and Baker–Campbell–Hausdorff product formulas. We show how this technique can be used to realize a number of operations of interest, including polynomials of annihilation and creation operators, i.e.,  $a^p a^{\dagger q}$  for integer  $p, q$ . We show examples of this paradigm including: obtaining universal control within a subspace of the entire Fock space of an oscillator, state preparation of a fixed photon number in the cavity, simulation of the Jaynes–Cummings Hamiltonian, simulation of the Hong–Ou–Mandel effect and more. This work demonstrates how techniques from Hamiltonian simulation can be applied to better control hybrid boson-qubit devices.

## 1 Introduction

Today, many quantum computing architectures are homogeneous – i.e. the same type of qubit is employed throughout the device. From devices made of superconducting qubits [1, 2, 3] to ion trap

---

\*These two authors contributed equally

qubits [4], prior work largely focuses on linking qubits of the same type together in fault-tolerant ways. However, there is a nascent body of work that studies the potential for hybrid quantum computers that leverage two or more types of quantum architectures (e.g., qubits and oscillator modes). These devices hold promise because they can be tailored for specific physical simulation problems, which would be especially useful in applications like material discovery or molecular simulation [5, 6] or quantum simulation of lattice models [7].

In particular, the hybrid qubit-boson (i.e., oscillator) models [8] hold some advantages. Specifically, the long lifetimes afforded to microwave photons in superconducting resonators have made them attractive targets for quantum error correction [8]. In addition, the Hilbert space accessible to a mode is much larger than that of qubits. Furthermore, the larger set of operations that can be performed by coupling an oscillator and a qubit open up the potential for multi-qubit interactions, such as the Mølmer-Sørensen gate [9] while at the same time enabling new forms of transduction between qubits and flying qubits such as photons [10, 11]. Oscillator interactions may also have unique features, like nonlinearities, which are challenging to simulate even with homogeneous quantum architectures [12].

However, whereas many useful applications have already been demonstrated with the experimentally available gate sets in ion traps and circuit QED, often problems of interest require more complex operations, and these must be compiled from the various experimental regimes and pulse sequences available. Specifically, techniques such as optimal control theory (OCT) [13, 14, 15] provide ways to design at a pulse level a sequence of controls that can be set in order to enact an arbitrary quantum transformation on a hybrid-boson qubit system. Although optimal control theory does provide a method of compiling nonnative operations into native gates, it is oftentimes intractable and almost always uninterpretable, yielding only a pulse which performs the desired operation without providing any physical intuition. Furthermore, it is computationally intensive to produce and due to the lack of theoretical understanding behind the pulse sequences it must be carried out on a case-by-case basis. These shortcomings further make models such as this difficult to program and to analyze the circuit complexity, as the procedure and in turn the cost for constructing an arbitrary unitary transformation can be difficult to bound.

Inspired by recent experimental progress [16, 17], we introduce in this paper an extensible control scheme for a hybrid boson-qubit quantum computer that is universal. Specifically, we consider the potential of instruction set architectures (ISAs) compiled from experimentally available gate sets using the Baker-Campbell-Hausdorff, Trotter-Suzuki and Lie-Trotter formulas. We develop two parallel approaches, one which primarily uses the creation and destruction operators which we refer to as based on ‘Fock methods’, and the other primarily relying on position and momentum operators which we refer to as based on ‘phase-space methods’. We demonstrate that both methods can be used to generate an ISA for bosonic devices. Furthermore, we use the previously mentioned formulas to realize a number of operations of interest, including polynomials of annihilation and creation operators, i.e.,  $a^p a^{\dagger q}$  for integer  $p, q$ . These block-encoded operations are crucial for QSP and certain problems in quantum simulation. Furthermore, we demonstrate that our compilation scheme obtains near-linear scaling and provide upper bounds on the maximum number of operations required to implement the compiled gate. Finally, we give examples for the Hamiltonian of a nonlinear material and applications to common unsolved problems in quantum simulation such as the Fermi-Hubbard model.

## 2 Preliminaries

In this section, we introduce the hybrid boson-qubit architecture we are operating on and the matrix product formulas we will use. The central goal of our work is to provide a generic toolbox that can be used to build unitary transformations on hybrid quantum devices that have both qubits as well as bosonic modes. Such devices are common in quantum computing, spanning circuit quantum electrodynamics (superconducting qubits coupled to microwave photons) to ion-trap quantum computing (for which the mechanical modes of oscillation are coupled to atomic qubits). The challenge though with these approaches is that fundamentally different insights are needed here to compile unitaries than the binary-based approaches that have been successful for the case of qubits.

Here we review the mathematical properties of bosonic quantum mechanics which are needed to understand the basic operations considered for the ISA architecture that we consider. Specifically, we present an analytic instruction set architecture (ISA) based on the Trotter-Suzuki and Baker-Campbell-Hausdorff (BCH) decompositions for decomposition of gates of the form  $U = e^{i\hat{H}\sigma^j}$ , where  $\hat{H}$  is a Hermitian operator composed of phase-space operators and Pauli gates. Before jumping into the specific details of our gate operations, we need to review the basics of bosonic quantum mechanics as well as the mathematical results needed to use these bosonic operations to compile a given unitary transformation.

### 2.1 A Hybrid Boson-Qubit Device

The central object that we need in this extension is the concept of a qumode, which stores the state of the bosons. Photons (energy quanta of the electromagnetic field) and phonons (quanta of mechanical vibrations) are examples of bosons present in current quantum computing experiments. Photons are the focus of photonic devices, cavity QED and hybrid circuit QED, whereas phonons are used to couple ion-spin qubits in ion traps. In the case of photons, the qumode stores the configuration of the electromagnetic field, and in the case of phonons, the qumode stores the vibrational state. We first produce a mathematical description of a qumode, then describe operations which can be performed on the qumode.

#### 2.1.1 Representing the qumode

There are two different bases that are commonly used to describe the state of the qumode:

1. *Phase-space representation*, where operators are written in terms of position ( $\hat{x}$ ) and momentum ( $\hat{p}$ ) operators
2. *Fock-space representation*, where operators are written in terms of bosonic creation ( $a^\dagger$ ) and annihilation ( $a$ ) operators.

In the phase-space representation, the computational basis corresponds to the strength of the electric field in the case of photons (or equivalently the position of a mechanical oscillator for vibrational systems). We refer to this with the operator  $\hat{x}$  and we have that for any  $x \in \mathbb{R}$ ,  $\hat{x}|x\rangle = x|x\rangle$ . It is often common to speak of the momentum operator  $\hat{p}$ , which can be found through the Fourier transform of  $\hat{x}$ . This describes the magnetic field for a photonic system. In practice, cutoffs are imposed on the values of the field and further discretization error on the gates and the outputs prevent arbitrary precision readout; however, for simplicity we ignore the latter issue in order to provide a simpler (if unrealistic) computational model and ignore the issue that

even when cutoffs are imposed the vector space does not strictly form a Hilbert space without also including spatial discretization.

In the Fock-space representation, we track the number of bosons (number of photons or the energy level of the harmonic oscillator for the vibrational case) in the computational basis. In this representation the computational basis is defined to be an eigenvector of the boson number operator  $\hat{n} |n\rangle = n |n\rangle$ , where  $\hat{n} = a^\dagger a$  is the number operator and  $a$  and  $a^\dagger$  add and remove a boson from the system, respectively. Formally this spectrum is countably infinite, but after truncation it forms a finite-dimensional Hilbert space and thus can be thought of as a qudit. For example, assuming a cutoff  $\Lambda = 3$ :

$$P_3 a^\dagger P_3 = \begin{bmatrix} 0 & 0 & 0 & 0 \\ 1 & 0 & 0 & 0 \\ 0 & \sqrt{2} & 0 & 0 \\ 0 & 0 & \sqrt{3} & 0 \end{bmatrix}, P_3 a P_3 = \begin{bmatrix} 0 & 1 & 0 & 0 \\ 0 & 0 & \sqrt{2} & 0 \\ 0 & 0 & 0 & \sqrt{3} \\ 0 & 0 & 0 & 0 \end{bmatrix}. \quad (1)$$

Here  $P_\Lambda$  is the projector onto the subspace of the cavity containing at most  $\Lambda$  photons, i.e.:

$$P_\Lambda : P_\Lambda |n\rangle = \begin{cases} |n\rangle & n \leq \Lambda \\ 0 & \text{otherwise} \end{cases}. \quad (2)$$

In this work, if unbounded operators are present, the remainder terms in the expansions that we consider become undefined and some form of a truncation is needed to ensure that the mathematics is well defined. Provided that an appropriate cutoff is picked for the system, the discrepancies between the truncated and untruncated systems will often be negligible. For notational clarity, we assume a cutoff of  $\Lambda$  for all further equations and assume the annihilation and creation operators implicitly have the projectors  $P_\Lambda$ .

The final aspect that we need to talk about in our description of the state is the qubits. In our model of computing we assume that the vector space is a tensor product of a qubit Hilbert space and the vector space of qumodes, i.e., the state space is  $\mathcal{H}_2 \otimes \mathcal{H}_\Lambda$ . This means that, for example, a computational basis state will be of the form  $|q\rangle \otimes |m\rangle_b$  where the state  $|q\rangle$  here can be thought of as the union of the qubit registers in the system, and  $|m\rangle_b$  represents a qumode state where the system is either in position  $x = m$  for the phase-space encoding or has  $m$  photons if the Fock-space encoding is used. Our work will assume only a single qubit register with a qumode in the Fock-space encoding.

### 2.1.2 Valid operations

Now that we have described the vector spaces that our operators act in, we will discuss the bosonic operations that act on the qumodes for the system. In order to introduce this, we need to review some notation surrounding bosonic creation and annihilation operators (otherwise known as raising and lowering or Fock operators). In the following, we demonstrate how some operations can be analytically decomposed, regardless of whether they are defined with Fock operators ( $a, a^\dagger$ ) or phase-space operators ( $\hat{x}, \hat{p}$ ), as these have the following equivalences:

$$\hat{x} = \frac{1}{2}(a + a^\dagger) \quad \Leftrightarrow \quad a = \hat{x} + i\hat{p}, \quad (3)$$

$$\hat{p} = -\frac{i}{2}(a - a^\dagger) \quad \Leftrightarrow \quad a^\dagger = \hat{x} - i\hat{p}, \quad (4)$$

and commutation relations:

$$[\hat{x}, \hat{p}] = \frac{i}{2}, \quad (5)$$

$$[a, a^\dagger] = 1. \quad (6)$$

There are many gate operations that can be considered as part of an instruction set. Within our ISA, operations can be qubit or qumode-exclusive or entangle across the qubit and qumode. For example, we can still perform single-qubit operations like  $H$  and  $R_z$ .

Additionally, we can assume that linear optical operations (which are at most quadratic in the field operators) can be performed on the modes, such as the displacement operations  $e^{\alpha a^\dagger + \alpha^* a}$  with  $\alpha$  a complex number, phase delays (or phase-space rotations)  $e^{-i\alpha a^\dagger a}$ , squeezing operations  $e^{\alpha a^2 - \alpha^* a^{\dagger 2}}$ , and beamsplitter operations  $e^{(aa^\dagger b - \alpha^* ab^\dagger)}$  where  $b$  is the creation operator acting on a different mode (although in this paper we are mainly interested in the single-mode case). We further assume that the qubit can be measured directly, but the oscillator can only be measured by entangling it with a qubit.

Finally, there are several entangling operations between oscillator and qubit that widely appear in the circuit QED literature. Two common ones are the controlled displacement operation [17]  $e^{-i(aa^\dagger + \alpha a) \otimes \sigma^z}$  and the Selective Number-dependent Arbitrary Phase (SNAP) gate [16]  $e^{-i \sum_n \alpha_n \hat{P}_n \otimes \sigma^z}$ , where  $\hat{P}_n = |n\rangle\langle n|$  is the projector onto the  $n$ th Fock state. (In our paper, we refer to hybrid gates with  $\sigma^i$  notation, while single-qubit gates like  $S, X, H$  are capitalized). Here, for convenience, we focus on a different gate, which we name  $\mathcal{S}_1$ , which we assume we can implement without error. While this gate can be approximated with arbitrary fidelity using conditional displacements (see Appendix A), in practice it can be implemented straightforwardly with OCT [18, 19, 20, 21].

**Definition 2.1.** For any  $t > 0$  and any positive integer cutoff  $\Lambda$ , we define  $\mathcal{S}_1$  to be the unitary acting on the Hilbert space  $\mathcal{H}_2 \otimes \mathcal{H}_\Lambda$  that has the following representation as a block-matrix

$$\mathcal{S}_1 = \exp \left( it \begin{bmatrix} 0 & a^\dagger \\ a & 0 \end{bmatrix} \right). \quad (7)$$

Notice that this gate operates simultaneously on the boson and qubit modes (producing, in the language of ion-trap quantum computers, a ‘red-sideband’ transition). In particular, the block-encoded matrix is equivalent to the following cavity-qubit coupling operator in the Jaynes-Cummings model:

$$\begin{bmatrix} 0 & a^\dagger \\ a & 0 \end{bmatrix} = |0\rangle\langle 1| \otimes a^\dagger + |1\rangle\langle 0| \otimes a. \quad (8)$$

The Jaynes-Cummings Hamiltonian is the natural one in circuit QED, therefore the coupling  $\mathcal{S}_1$  is naturally present. However, one can choose an experimental parameter regime in which the coupling becomes negligible. This happens when the cavity and qubit are strongly detuned, and they obey the dispersive coupling Hamiltonian. This is a useful regime, which may be chosen, for example, when needing to use the controlled displacement gate. The  $\mathcal{S}_1$  block encoding can be synthesized in this regime, and this is demonstrated in Appendix A.

The reason why we focus on this incredibly simple example is to provide a case that is likely to have an advantage in our hybrid model. Specifically, the further we are away from the natural interactions that are present in our quantum simulator the more expensive we anticipate a simulation to be, as we will have to construct the desired interaction from a potentially long sequence of

fundamental interactions. In this sense, our approach borrows inspiration from analog simulation. Unlike analog simulation, the interactions here are universal in the sense that we can emulate *any Jaynes-Cummings model* using our approach.

## 2.2 Lie product formulas

Lie product formulas describe the behavior when matrix exponentials are multiplied, i.e., how  $e^A e^B$  behaves. These formulas are well-known in Hamiltonian simulation [22, 23, 24] and are used to approximate a discretized version of the time evolution operator  $e^{-iHt}$  using the Trotter formula. However, in our application, we demonstrate how these formulas can be used as a control scheme for our device.

We introduce two product formulas: the Baker-Campbell-Hausdorff (BCH) formula and the Lie-Trotter formula. The BCH formula can be used to create a commutator (or anticommutator) of operators. The Trotter formula can be used to add these commutators/anticommutators together. We introduce the informal theorems below:

**Theorem 2.2** (Informal BCH theorem from [25]). *Suppose we can implement the operators  $e^{A\lambda}, e^{B\lambda}$  for  $\lambda \in \mathbb{R}$ . Then, a BCH formula of order  $p$  has the following error scaling:*

$$\text{BCH}_p(A\lambda, B\lambda) = e^{A\lambda} e^{B\lambda} e^{-A\lambda} e^{-B\lambda} \quad (9)$$

$$= e^{[A,B]\lambda^2} + \mathcal{O}((\max(\|A\|, \|B\|)\lambda)^{2p+1}), \quad (10)$$

requiring no more than  $8 \cdot 6^{p-1}$  exponentials.

**Theorem 2.3** (Informal Trotter theorem from [23]). *Suppose we may implement  $e^{A\lambda}$  and  $e^{B\lambda}$  for arbitrary  $\lambda \in \mathbb{R}$ . Then, a  $p^{\text{th}}$  order Trotter formula has the following error scaling:*

$$\text{Trotter}_{2p}(A\lambda, B\lambda) = e^{(A+B)\lambda} + \mathcal{O}((\|A+B\|\lambda)^{2p+1}), \quad (11)$$

requiring no more than  $4 \cdot 5^{p-1}$  exponentials.

Though the BCH formula is defined only to produce commutators, we can use our qubit to produce anticommutators of bosonic operations. Informally, we exploit commutators of Pauli operations to create a phase change, as  $\sigma^z = -\frac{i}{2}[\sigma^x, \sigma^y]$ . Thus, BCH can be used to create an anticommutation relation on the mode operators

$$i[iA\sigma^x, iB\sigma^y] = \{A, B\}\sigma^z. \quad (12)$$

We later show how these commutators and anticommutators can be combined to directly implement products of operators. Observing that  $\frac{1}{2}[A, B] + \frac{1}{2}\{A, B\} = AB$ , we can use the Trotter formula to produce:

$$\text{Trotter} \left( \frac{1}{2}[A, B], \frac{1}{2}\{A, B\} \right) \approx \exp(AB). \quad (13)$$

## 3 Producing Anticommutators and Exponential Products

In this section, we formalize our technique and present methods for both hermitian operators, such as phase-space operators  $\hat{x}$  and  $\hat{p}$ , and non-hermitian operators, such as Fock space operators  $a, a^\dagger$ . We examine the task of constructing polynomials in phase space as well as Fock space operators using qubit controlled operations. We first show how the additional qubit of our hybrid boson-qubit

Formula	Target	Preconditions	Reference
BCH( $\exp itB\sigma^i, \exp itA\sigma^i$ )	$\exp(t^2[A, B])\mathbf{1}$	$A, B$ Hermitian	<a href="#">Theorem 2.2</a>
BCH( $\exp itA\sigma^j, \exp itB\sigma^k$ )	$\exp(-it^2\{A, B\}\sigma^i)$	$A, B$ Hermitian	<a href="#">Equation (12)</a>
BCH( $X\mathcal{B}_B(t)X, \mathcal{B}_A(t)$ )	$\exp(t^2(AB - (AB)^\dagger)\sigma^z)$	$[A, B] = 0$	<a href="#">Equation (39)</a>
BCH( $S\mathcal{B}_A(t)S^\dagger, X\mathcal{B}_B(t)X$ )	$\exp(it^2(AB + (AB)^\dagger)\sigma^z)$	$[A, B] = 0$	<a href="#">Equation (40)</a>
BCH( $S\mathcal{B}_A(t)S^\dagger, X\mathcal{B}_B(t)X$ )	$\exp(2it^2AB\sigma^z)$	$[A, B] = 0,$ $AB = (AB)^\dagger$	<a href="#">Equation (41)</a>
Trotter( $\exp t(AB - (AB)^\dagger)\sigma^y,$ $\exp it(AB + (AB)^\dagger)\sigma^x$ )	$\exp\left(2it \begin{bmatrix} 0 & BA \\ AB & 0 \end{bmatrix}\right)$	$[A, B] = 0$	<a href="#">Theorem 3.1</a>
BCH( $S\mathcal{B}_B(t)S^\dagger, X\mathcal{B}_A(t)X$ )	$\exp\left(it \begin{bmatrix} 2AB & 0 \\ 0 & -BA - (BA)^\dagger \end{bmatrix}\right)$	$AB = (AB)^\dagger$	<a href="#">Theorem 3.2</a>

Table 1: Overview of techniques for synthesizing particular unitary transformations and the quantum gates needed in order to build the constructs proposed in this paper. Each row contains the formula used, the target to approximate, the preconditions, and a reference to the location of the precise statement of the performance of the method. The formula provided denotes hybrid gates with  $\sigma^i$  terms, while single-qubit gates are capitalized (e.g.,  $S, X, H$ ). The bounds on the number of gates depend on the accuracy required of the approximation and are given in the corresponding theorems.

architecture allows for the synthesis of anticommutators of hermitian operators and, by proxy, matrix products of phase-space operators. We then use similar techniques with non-hermitian operators such as Fock-space operators to manipulate block encodings of matrices. Finally, we contextualize these methods with asymptotic error bounds, providing theoretical analyses of our proposed techniques.

We denote block-encoded matrices with the following notation:

$$\mathcal{B}_A = \exp it \begin{bmatrix} 0 & A \\ A^\dagger & 0 \end{bmatrix}, \quad (14)$$

where the subscript is the upper right block and the lower left block is the transpose and complex conjugate to preserve hermiticity. This block encoded gate corresponds to  $\exp itA\sigma^x$  only if  $A$  is hermitian, otherwise it corresponds to  $\exp it(|0\rangle\langle 1| \otimes A^\dagger + |1\rangle\langle 0| \otimes A)$ , the synthesis of which we show in [Appendix A](#).

### 3.1 Phase-space methods: anti-commutators of Hermitian operators

Here, we demonstrate how to synthesize anti-commutation relations between Hermitian operators, as is the case for the phase space operators  $\hat{x}$  and  $\hat{p}$  (but not Fock space operators). To do this, we use qubit gates to introduce the phase change necessary for obtaining an anticommutator. These methods can be used to generate beamsplitters and the Hong-Ou Mandel effect, as is explored in [Section 4](#).

Our technique applies the BCH formula on a hybrid boson-qubit operation. Thus, we need to study how the commutator affects both bosonic and qubit operators. In the bosonic case, observe:

$$[\hat{x}, \hat{p}] = \frac{i}{2}. \quad (15)$$

In the qubit case, observe that:

$$\sigma^i = \epsilon_{ijk} \frac{i}{2} [\sigma^j, \sigma^k], \quad (16)$$

$$(17)$$

where  $\epsilon_{ijk}$  is the Levi-Civita symbol, and  $i, j, k \in \{x, y, z\}$ .

We use these relations, as well as the Pauli product identity

$$\sigma^i = \epsilon_{ijk} i \sigma^j \sigma^k. \quad (18)$$

to enable the expression of the product of a single Pauli operator and an anticommutator  $\{A, B\} \sigma_i$  in terms of the product of modes and single Pauli operators in the form of a commutator, as follows:

$$\{A, B\} \sigma^i = AB (i\sigma^j \sigma^k) + BA (i\sigma^k \sigma^j) \quad (19)$$

$$= i \left( - (A\sigma^j) (B\sigma^k) + BA (\sigma^k \sigma^j) \right) \quad (20)$$

$$= i \left( (iA\sigma^j) (iB\sigma^k) - (iB\sigma^k) (iA\sigma^j) \right) \quad (21)$$

$$= i [iA\sigma^j, iB\sigma^k]. \quad (22)$$

assuming  $A$  and  $B$  are Hermitian, and commute with  $\sigma^i$  as is the case when  $A, B$  are mode-only operators. Thus, by using a hybrid qubit-cavity operation of the form  $\exp iA\sigma^j, \exp iB\sigma^k$ , with  $A$  and  $B$  Hermitian, the BCH formula can convert commutators into anticommutators.

### 3.2 Fock methods - non-linear terms via block-encodings

In this section, we show how to achieve  $A^q$  for an arbitrary bosonic operator  $A$ . This extends the prior techniques, which required that  $A$  be Hermitian. When  $A$  is a Fock space operator, this corresponds to realizing arbitrary powers of  $a$  and  $a^\dagger$ , which is known to generate a universal set of operations on the bosonic modes. This is useful for the simulation of non-linear materials which naturally lead to terms that are polynomial in the creation and annihilation operators, as well as quantum signal processing [26], for example.

Our method again uses the qubit coupling to induce a phase in the compound qubit-boson system, similar to the previous section. We begin with block-encodings as described in Eq. 14. First, we show how to create auxiliary block encodings via qubit-only gates, a technique known as conjugation. Second, we show how to generate squeezing and non-linear terms using the BCH formula. Third, we note that qubit rotations lead to quadratic block encodings. Fourth, we show that these methods may be extended to multiple Hilbert spaces. Finally, we present a formal algorithm and associated error bound to attain these block-encodings.

To manipulate the block-encodings, begin by recognizing that qubit-only operations can modify the exponential via “conjugation”:

$$U e^A U^\dagger = e^{U A U^\dagger}. \quad (23)$$

Thus, given any block-encoding, we can also create the following auxiliaries:

$$X \exp it \begin{bmatrix} 0 & A \\ A^\dagger & 0 \end{bmatrix} X = \exp it \begin{bmatrix} 0 & A^\dagger \\ A & 0 \end{bmatrix}, \quad (24)$$

$$S \exp it \begin{bmatrix} 0 & A \\ A^\dagger & 0 \end{bmatrix} S^\dagger = \exp it \begin{bmatrix} 0 & -iA \\ iA^\dagger & 0 \end{bmatrix}, \quad (25)$$



where  $S$  is a qubit phase gate. Applying BCH yields the following commutators:

$$[X\mathcal{B}(t)X, \mathcal{B}(t)] = \left[ it \begin{bmatrix} 0 & A^\dagger \\ A & 0 \end{bmatrix}, it \begin{bmatrix} 0 & A \\ A^\dagger & 0 \end{bmatrix} \right] = -t^2 \left( \begin{bmatrix} (A^\dagger)^2 & 0 \\ 0 & A^2 \end{bmatrix} - \begin{bmatrix} A^2 & 0 \\ 0 & (A^\dagger)^2 \end{bmatrix} \right) \quad (26)$$

$$= t^2 \sigma^z \otimes (A^2 - (A^\dagger)^2), \quad (27)$$

$$[S\mathcal{B}(t)S^\dagger, X\mathcal{B}(t)X] = \left[ it \begin{bmatrix} 0 & -iA \\ iA^\dagger & 0 \end{bmatrix}, it \begin{bmatrix} 0 & A^\dagger \\ A & 0 \end{bmatrix} \right] = -t^2 \left( \begin{bmatrix} -iA^2 & 0 \\ 0 & i(A^\dagger)^2 \end{bmatrix} - \begin{bmatrix} i(A^\dagger)^2 & 0 \\ 0 & -iA^2 \end{bmatrix} \right) \quad (28)$$

$$= it^2 \sigma^z \otimes (A + (A^\dagger)^2). \quad (29)$$

These commutators themselves can be conjugated. Recall that  $HZH = X$  and  $SHZHS^\dagger = Y$ :

$$SH[X\mathcal{B}(t)X, \mathcal{B}(t)]HS^\dagger = t^2 \sigma^y \otimes (A^2 - (A^\dagger)^2), \quad (30)$$

$$H[S\mathcal{B}(t)S^\dagger, X\mathcal{B}(t)X]H = it^2 \sigma^x \otimes (A + (A^\dagger)^2), \quad (31)$$

so that:

$$it^2 \sigma^x \otimes (A + (A^\dagger)^2) + t^2 \sigma^y \otimes (A^2 - (A^\dagger)^2) = 2it^2 \begin{bmatrix} 0 & (A^\dagger)^2 \\ A^2 & 0 \end{bmatrix}. \quad (32)$$

This approach can also be extended to cases where the constituent operators are of different types, e.g. when the synthesized unitary operates on two different modes, as in the conditional beamsplitter which is a gate that acts as a beamsplitter controlled on an ancillary qubit. For example, consider the following commutator:

$$\left[ i\tau \begin{bmatrix} 0 & B^\dagger \\ B & 0 \end{bmatrix}, i\tau \begin{bmatrix} 0 & A \\ A^\dagger & 0 \end{bmatrix} \right] = -\tau^2 \left( \begin{bmatrix} B^\dagger A^\dagger & 0 \\ 0 & BA \end{bmatrix} - \begin{bmatrix} AB & 0 \\ 0 & A^\dagger B^\dagger \end{bmatrix} \right) \quad (33)$$

$$= \tau^2 \begin{bmatrix} AB - (AB)^\dagger & 0 \\ 0 & (BA)^\dagger - BA \end{bmatrix}, \quad (34)$$

$$\left[ i\tau \begin{bmatrix} 0 & -iA \\ iA^\dagger & 0 \end{bmatrix}, i\tau \begin{bmatrix} 0 & B^\dagger \\ B & 0 \end{bmatrix} \right] = -\tau^2 \left( \begin{bmatrix} -iAB & 0 \\ 0 & iA^\dagger B^\dagger \end{bmatrix} - \begin{bmatrix} iB^\dagger A^\dagger & 0 \\ 0 & -iBA \end{bmatrix} \right) \quad (35)$$

$$= i\tau^2 \begin{bmatrix} AB + (AB)^\dagger & 0 \\ 0 & -BA - (BA)^\dagger \end{bmatrix}. \quad (36)$$

Observe that when  $[A, B] = 0$ , as is the case when  $A, B$  are both annihilation/creation operators or when they act on different modes, we can rewrite the commutators in the following forms:

$$\left[ i\tau \begin{bmatrix} 0 & B^\dagger \\ B & 0 \end{bmatrix}, i\tau \begin{bmatrix} 0 & A \\ A^\dagger & 0 \end{bmatrix} \right] = -\tau^2 \begin{bmatrix} AB - (AB)^\dagger & 0 \\ 0 & (AB)^\dagger - AB \end{bmatrix} = \tau^2 (AB - (AB)^\dagger) \sigma^z, \quad (37)$$

$$\left[ i\tau \begin{bmatrix} 0 & -iA \\ iA^\dagger & 0 \end{bmatrix}, i\tau \begin{bmatrix} 0 & B^\dagger \\ B & 0 \end{bmatrix} \right] = i\tau^2 \begin{bmatrix} AB + (AB)^\dagger & 0 \\ 0 & -AB - (AB)^\dagger \end{bmatrix} = i\tau^2 (AB + (AB)^\dagger) \sigma^z, \quad (38)$$

so that, again:

$$SH\tau^2 (AB - (AB)^\dagger) \sigma^z HS^\dagger = \tau^2 (AB - (AB)^\dagger) \sigma^y, \quad (39)$$

$$Hi\tau^2 (AB + (AB)^\dagger) \sigma^z H = i\tau^2 (AB + (AB)^\dagger) \sigma^x. \quad (40)$$

---

**Algorithm 1** ADD( $\mathcal{B}_A(t), \mathcal{B}_B(t), p_l, p_r, t$ )

---

**Input:**  $[A, B] = 0$ ,  $\left\| \mathcal{B}_A - \exp it \begin{bmatrix} 0 & A \\ A^\dagger & 0 \end{bmatrix} \right\| \in \mathcal{O}((c_A t)^{p_A})$ ,  $\left\| \mathcal{B}_B - \exp it \begin{bmatrix} 0 & B \\ B^\dagger & 0 \end{bmatrix} \right\| \in \mathcal{O}((c_B t)^{p_B})$ ,  
 $p_A, p_B \geq 1, t > 0$

**Output:**  $\mathcal{B}_{AB}$  where  $\left\| \mathcal{B}_{AB}(t) - \exp it \begin{bmatrix} 0 & AB \\ (AB)^\dagger & 0 \end{bmatrix} \right\| \in \mathcal{O}((Ct)^{\min(p_A, p_B)/2})$  for constant  $C$

$$q := \max(\lceil \frac{1}{2}(\min(p_l, p_r) - 1) \rceil, 1)$$

$$s := \max(\lceil \frac{1}{2}(\min(p_l, p_r) - 1) \rceil, 1)$$

$$\tau := \sqrt{t/2}$$

$$\text{Left} := \text{BCH}_{q,1}(X \cdot \mathcal{B}_B(t) \cdot X, \mathcal{B}_A(t))$$

$$\text{Right} := \text{BCH}_{q,1}(S \cdot \mathcal{B}_A(t) \cdot S^\dagger, X \cdot \mathcal{B}_B(t) \cdot X)$$

$$\text{Left}' := SH \cdot \text{Left} \cdot HS^\dagger$$

$$\text{Right}' := H \cdot \text{Right} \cdot H$$

**return**  $X \cdot \text{Trotter}_s(\text{Left}', \text{Right}') \cdot X$

---

Via Trotter, we can finally implement the sum:

$$\tau^2(AB - (AB)^\dagger)\sigma^y + i\tau^2(AB + (AB)^\dagger)\sigma^x = 2i\tau^2 \begin{bmatrix} 0 & (AB)^\dagger \\ AB & 0 \end{bmatrix}. \quad (41)$$

Finally, we select  $\tau = \sqrt{\frac{t}{2}}$  to obtain the desired time and conjugate by  $\sigma^x$  to produce the desired matrix. Observe that [Algorithm 1](#) thus yields  $\mathcal{B}_{AB}$ , provided that  $[A, B] = 0$ . This process can be repeated iteratively, assuming  $AB$  commutes with  $B$ ; for example, if  $A = B = a$ , then this process can be used to produce higher powers  $a^k, (a^\dagger)^k$  of the annihilation / creation operators.

[Algorithm 1](#) is an extension of the prior commutator approaches in phase space because the  $\sigma^i = -\frac{i}{2}[\sigma^j, \sigma^k]$  relation is natively expressed in the algorithm; i.e., if we have  $\mathcal{B}_A = \mathcal{B}_B = \mathcal{B}_{\hat{x}} = \exp it \hat{x} \sigma^x$ , the ‘‘Left’’ term vanishes and the ‘‘Right’’ term is the commutator we would apply.

Finally, in [Algorithm 2](#), we demonstrate how to implement  $AB$  if  $AB = (AB)^\dagger$ . This process cannot be performed recursively, contrary to [Algorithm 1](#), because it places the terms in the upper-left block encoding. However, this actually may be more useful, as it allows the precise simulation of  $e^{iABt}$ , assuming the qubit begins in the  $|0\rangle$  state:

$$\left[ i\tau \begin{bmatrix} 0 & -iB^\dagger \\ iB & 0 \end{bmatrix}, i\tau \begin{bmatrix} 0 & A \\ A^\dagger & 0 \end{bmatrix} \right] = \tau^2 \begin{bmatrix} iB^\dagger A^\dagger + iAB & 0 \\ 0 & -iBA - iA^\dagger B^\dagger \end{bmatrix} \quad (42)$$

$$= i\tau^2 \begin{bmatrix} 2AB & 0 \\ 0 & -BA - (BA)^\dagger \end{bmatrix}. \quad (43)$$

### 3.3 Error analysis

The prior description of our algorithm assumes error-less product formulas. However, the BCH and Trotter formulas actually introduce errors which must be accounted for, especially when applying our algorithm recursively. In this section, we cite the error scaling of the general addition algorithm described in [Algorithm 1](#) and the multiplication algorithm described in [Algorithm 2](#). The proofs and full results are included in [Appendix B](#).

---

**Algorithm 2**  $MULT(\mathcal{B}_A(t), \mathcal{B}_B(t), p_l, p_r, t)$ 


---

**Input:**  $AB = (AB)^\dagger$ ,  $p_l, p_r \geq 1$ ,  $t > 0$

**Output:** An upper-left block encoding  $\mathcal{M}_{AB}$  where  $\left\| \mathcal{M}_{AB}(t) - \exp it \begin{bmatrix} AB & 0 \\ 0 & \frac{1}{2}(-BA - (BA)^\dagger) \end{bmatrix} \right\| \in \mathcal{O}((C^2 t)^{\min(p_A, p_B)/2})$  for constant  $C$   
 $q := \max(\lceil \frac{1}{2}(\min(p_l, p_r) - 1) \rceil, 1)$   
 $\tau := \sqrt{t/2}$   
**return**  $BCH_q(S\mathcal{B}_B(\tau)S^\dagger, X\mathcal{B}_A(\tau)X)$

---

**Theorem 3.1.** *Suppose we have approximations  $\tilde{\mathcal{B}}_A(t), \tilde{\mathcal{B}}_B(t)$  with the following error scaling:*

$$\left\| \tilde{\mathcal{B}}_A(t) - \mathcal{B}_A(t) \right\| \in \mathcal{O}((ct)^{p_A}), \quad (44)$$

$$\left\| \tilde{\mathcal{B}}_B(t) - \mathcal{B}_B(t) \right\| \in \mathcal{O}((ct)^{p_B}), \quad (45)$$

for some constant  $c$  and order  $p_A, p_B \geq 1$  where  $[A, B] = 0$ . Then, the application of [Algorithm 1](#) will yield the following scaling:

$$\left\| ADD(\tilde{\mathcal{B}}_A(t), \tilde{\mathcal{B}}_B(t)) - \exp it \begin{bmatrix} 0 & AB \\ BA & 0 \end{bmatrix} \right\| \in \mathcal{O}\left((C_{TOTAL}t)^{\min(p_A, p_B)/2}\right), \quad (46)$$

with  $C_{TOTAL} = \max(\|AB\|, \|BA\|, C_{BCH}^2)$  and  $C_{BCH} = \max(\|A\|, \|B\|, c)$ , using no more than  $1.07 \cdot 30^q$  exponentials, where  $q = \max(\lceil \frac{\min(p_1, p_2) - 1}{2} \rceil, 1)$ .

**Theorem 3.2.** *Suppose we have some approximate block encodings  $\tilde{\mathcal{B}}_A, \tilde{\mathcal{B}}_B$  with the following error:*

$$\left\| \tilde{\mathcal{B}}_A(t) - \exp it \begin{bmatrix} 0 & A \\ A^\dagger & 0 \end{bmatrix} \right\| \in \mathcal{O}((ct)^{p_A}), \quad (47)$$

$$\left\| \tilde{\mathcal{B}}_B(t) - \exp it \begin{bmatrix} 0 & B \\ B^\dagger & 0 \end{bmatrix} \right\| \in \mathcal{O}((ct)^{p_B}), \quad (48)$$

for constant  $c$  and  $p_A, p_B \geq 1$  where  $AB = (AB)^\dagger$ . Then, [Algorithm 2](#) has the following error:

$$\left\| MULT(\tilde{\mathcal{B}}_A(t), \tilde{\mathcal{B}}_B(t)) - \exp it \begin{bmatrix} AB & 0 \\ 0 & \frac{1}{2}(-BA - (BA)^\dagger) \end{bmatrix} \right\| \in \mathcal{O}\left((C^2 t)^{\min(p_A, p_B)/2}\right), \quad (49)$$

with  $C = \max(\|A\|, \|B\|, c)$ , using no more than  $8 \cdot 6^{q-1}$  exponentials where  $q = \max(\lceil \frac{\min(p_A, p_B) - 1}{2} \rceil, 1)$ .

While the asymptotic error analysis suggests that the cost of this method is onerous, we note that the product formulas often have overly pessimistic error scaling and operation counts [27]. In the applications below, we provide numerical simulations which suggest our technique is more readily implementable than theory suggests.

## 4 Applications

In this section, we show how our technique is a powerful tool for analytically realizing desired operations. This technique not only works for Hamiltonian simulation problems, but also for general

control problems. In particular, we show how the physical intuition for a desired transformation is often sufficient to produce an approach to create desired operations.

We introduce applications in both phase- and Fock-space. Phase-space techniques may be useful in the case where, for example, displacements ( $e^{(\alpha a^\dagger + \alpha^* a)} = e^{i\alpha \vec{x}}$  for  $\alpha$  real or  $e^{i\alpha \vec{p}}$  for  $\alpha$  imaginary) are the only experimentally available gates. We combine these position  $\vec{x}$  and momentum  $\vec{p}$  operators with single-qubit rotations  $\vec{\sigma}$  to produce the phase-space rotation operator, earlier referred to as the controlled parity operator,  $e^{ia^\dagger a \sigma^z t}$ ; the beamsplitter  $e^{-i\sigma^z (a^\dagger b + ab^\dagger)t}$ ; gates for two encodings of universal control of the restricted span $\{|0\rangle, |1\rangle\}$  Hilbert space (Appendix E); and gates for simulation of Fermi-Hubbard lattice dynamics using the vacuum and 1<sup>st</sup> Fock states of the cavity (Appendix F), including same-site, hopping, controlled-beamsplitter (Appendix C.2), and FSWAP gates. For applications in Fock space, we use qubit-controlled displacements  $e^{\sigma^z (\alpha^* a + \alpha a^\dagger)}$ , controlled parity maps  $e^{\sigma^z a^\dagger a}$  and single-qubit operations  $\vec{\sigma}$  to produce polynomials of annihilation and creation operators, i.e.,  $a^p a^{\dagger q}$  for integer  $p, q$ . We then demonstrate how polynomials of these operators can be used in Hamiltonian simulation (e.g. with  $\chi^{(3)}$  nonlinear materials, Appendix D.2) and state preparation (Appendix D.3).

#### 4.1 Nonlinear Hamiltonian simulation

As a simple application, let us consider the case of simulating a  $\chi^{(3)}$  nonlinear material. These interactions commonly occur in nonlinear optics and appear when the index of refraction for a material varies linearly with the intensity of the electromagnetic field. Such interactions can be modeled for a single mode using the following expression

$$H = \omega a^\dagger a + \frac{\kappa}{2} (a^\dagger)^2 a^2. \quad (50)$$

Our goal here is to examine the cost of a simulation of such a Hamiltonian in our model for time  $t$  and error tolerance  $\epsilon$  and determine the parameter regimes within which a hybrid simulation using our techniques could provide an advantage with respect to a conventional qubit-based simulation of the Hamiltonian.

Each of the terms can be approximated by using the BCH formula. For the  $\omega a^\dagger a$  term, observe that we can approximate this term with a single application of the BCH formula. Namely,

$$\left[ i\tau_1 \begin{bmatrix} 0 & -ia^\dagger \\ ia & 0 \end{bmatrix}, i\tau_1 \begin{bmatrix} 0 & a^\dagger \\ a & 0 \end{bmatrix} \right] = 2i\tau_1^2 \begin{bmatrix} a^\dagger a & 0 \\ 0 & -aa^\dagger \end{bmatrix}, \quad (51)$$

where the first matrix corresponds to  $\mathcal{S}_1^y = S \cdot \mathcal{S}_1 \cdot S^\dagger$  operator and the second matrix corresponds to  $\mathcal{S}_1$  operator. Similarly, observe that:

$$\left[ i\tau_2 \begin{bmatrix} 0 & -i(a^\dagger)^2 \\ ia^2 & 0 \end{bmatrix}, i\tau_2 \begin{bmatrix} 0 & (a^\dagger)^2 \\ a^2 & 0 \end{bmatrix} \right] = 2i\tau_2^2 \begin{bmatrix} (a^\dagger)^2 a^2 & 0 \\ 0 & -a^2 (a^\dagger)^2 \end{bmatrix}. \quad (52)$$

Thus, via BCH formula, we can block-encode the two Hamiltonian terms. Applying Trotterization allows us to block-encode the entire Hamiltonian into the upper-left quadrant. Thus, by setting the qubit to  $|0\rangle$ , we can approximate the Hamiltonian. The error scaling is as follows and is proven in Appendix D.2

**Theorem D.4.** *Let  $H = \omega a^\dagger a + \frac{\kappa}{2} (a^\dagger)^2 a^2$ ,  $t$  be an evolution time and  $\epsilon$  be an error tolerance. For any positive integer  $q$  we can approximate an exponential of the block-encoded Hamiltonian with error at most  $\epsilon$  in the operator norm using  $r e^{\mathcal{O}(q)} \mathcal{S}_1$  operations where  $r \in \Omega \left( \frac{(\Lambda^4 t)^{1+1/(q-\frac{3}{4})}}{\epsilon^{1/(q-\frac{3}{4})}} \right)$ .*

This shows that we can perform a simulation of the dynamics within error  $\epsilon$  using a number of operations within our instruction set that scales near-linearly with the evolution time and sub-polynomially with  $\epsilon$ . Further, this approach requires no ancillary memory and can be done with a single oscillator and a qubit. This is a dramatic memory reduction relative to the quantum case, which requires a polylogarithmic number of qubits in  $\Lambda$ .

It is worth noting that in this case the ancillary qubit is not being used directly in the model. Instead it is being used to control the dynamics and generate the appropriate nonlinear interaction between the photons present in the model.

## 4.2 Nondestructive measurement of the qumode

We now demonstrate how the approach can extend beyond problems in Hamiltonian simulation. We begin with an example of the technique for control. In particular, we seek to perform a nondestructive measurement of the qumode. Natively, measurements are destructive, i.e., counting the number of photons also consumes the photons. However, by using the qubit, we can instead project the information into the qubit [28, 29].

Intuitively, we seek to implement  $e^{it\hat{n}\sigma^z}$  where  $\hat{n} = a^\dagger a$  is the number operator. If we could implement this gate for arbitrary  $t$ , we could perform phase estimation on the qubit to nondestructively project the qumode into a fixed number of bosons. This could be done by setting  $t$  sufficiently small so that  $t\Lambda \leq 2\pi$  is calculable with phase estimation. Alternatively, for  $t = \pi$ , this operation checks the parity of the qumode and applies an RZ gate for odd parities. We employ the instruction set in the phase-space representation to synthesize the infinitesimal conditional rotation gate

$$U_{\text{rot},k} = e^{i\lambda^2 \hat{n} \sigma^k} \quad (53)$$

for  $k = x, y, z$ . We rewrite  $\hat{n}$  in terms of the phase-space operators by recognizing:

$$\hat{n} = \hat{a}^\dagger \hat{a} \quad (54)$$

$$= \hat{x}^2 + \hat{p}^2 - \frac{1}{2}. \quad (55)$$

Thus, by applying Eq. 55, Eq. 4, and Eq. 3 yields

$$i\lambda^2 \hat{n} \sigma^k = i \left( \hat{x}^2 + \hat{p}^2 - \frac{1}{2} \right) \sigma^k \lambda^2, \quad (56)$$

such that the gate is expressed via the Trotter-Suzuki decomposition as the product of  $\exp([A_1, B_1]) = \exp(i\lambda^2 \hat{x}^2 \sigma^k)$ ,  $\exp([A_2, B_2]) = \exp(i\lambda^2 \hat{p}^2 \sigma^k)$ , and conditional displacement  $\exp(-i\lambda^2 \sigma^k / 2)$ . Given the Pauli commutator relation, the first commutator is

$$[A_1, B_1] = i\hat{x}^2 \sigma^k \quad (57)$$

$$= i\hat{x}^2 \left( -\frac{i}{2} [\sigma^i, \sigma^j] \right) \quad (58)$$

$$= \left[ \frac{1}{\sqrt{2}} \hat{x} \sigma^i, \frac{1}{\sqrt{2}} \hat{x} \sigma^j \right], \quad (59)$$

and the second commutator is

$$[A_2, B_2] = i\hat{p}^2 \sigma^k \quad (60)$$

$$= i\hat{p}^2 \left( -\frac{i}{2} [\sigma^i, \sigma^j] \right) \quad (61)$$

$$= \left[ \frac{1}{\sqrt{2}} \hat{p} \sigma^i, \frac{1}{\sqrt{2}} \hat{p} \sigma^j \right], \quad (62)$$

such that both terms are amenable to BCH decomposition, and the infinitesimal conditional rotation is composed with a gate-depth lower bound of nine. To perform an error analysis, we may directly apply the error scaling of BCH and Trotter to find:

**Theorem C.1.** *Suppose we can implement  $e^{it\hat{x}\sigma^i}$ ,  $e^{it\hat{p}\sigma^i}$  without error. Then, we may approximate  $\mathcal{B}_{\hat{x}^2+\hat{p}^2}$  with arbitrary error scaling  $p$ :*

$$\left\| \tilde{\mathcal{B}}_{\hat{x}^2+\hat{p}^2} - \mathcal{B}_{\hat{x}^2+\hat{p}^2} \right\| \in \mathcal{O}((Ct)^{p+1/2}), \quad (118)$$

where  $C = \max(\|\hat{x}^2 + \hat{p}^2\|, \|\hat{x}\|^2, \|\hat{p}\|^2)$  and using no more than  $4 \cdot 5^{\frac{p}{2}-\frac{1}{4}}$  exponentials.

We then provide numerics in [Figure 1](#). As expected, the wavefunction initialized in the second excited state of the cavity and the ground state of the associated transmon has an autocorrelation function that oscillates with phase  $\exp(2it)$ . Dynamics are well reproduced with 2000 time steps for a final time of 20 with 15 states in the cavity. Note the units are arbitrary in the absence of definition of the cavity frequency  $\omega$ , with the only units defined by setting the reduced Planck constant to unity  $\hbar = 1$  arb. units. The close agreement between the BCH-synthesized and exact gates is supported by the error scaling after a single gate application computed for time step  $t$ , which features a power law scaling in agreement with the predicted error scaling for both BCH and Trotter decompositions.

We can obtain a similar decomposition with Fock-space operators. Observe that the MULT subroutine applied to the  $\mathcal{B}_a, \mathcal{B}_{a^\dagger}$  would yield the following operators:

$$\left\| \text{MULT}(\mathcal{B}_a, \mathcal{B}_{a^\dagger}) - \exp it \begin{bmatrix} a^\dagger a & 0 \\ 0 & -aa^\dagger \end{bmatrix} \right\|. \quad (63)$$

Note that  $aa^\dagger = a^\dagger a + \mathbf{1}$  provided we understand this operator to be acting on vectors that have no support on the singularity, so the block encoding that is actually applied is actually the following:

$$\exp it \left\{ \begin{bmatrix} a^\dagger a & 0 \\ 0 & -a^\dagger a \end{bmatrix} + \begin{bmatrix} 0 & 0 \\ 0 & -\mathbf{1} \end{bmatrix} \right\} = \exp it(\hat{n}\sigma^z - \mathbf{1}_\gamma(\mathbf{1} - \sigma^z)). \quad (64)$$

Thus, our Fock-space methods would also achieve the same transformation, albeit requiring a phase and RZ correction.

### 4.3 State preparation from the vacuum

Consider the case where we seek to prepare  $|k\rangle_b$  on the qumode. On qubit devices, this sort of state prep is trivial, assuming the qubits represent logic in a binary fashion. However, hybrid boson-qubit devices natively implement exponentials of the phase-space or Fock-space operators. Thus, preparing  $|k\rangle_b$  directly can often be challenging.

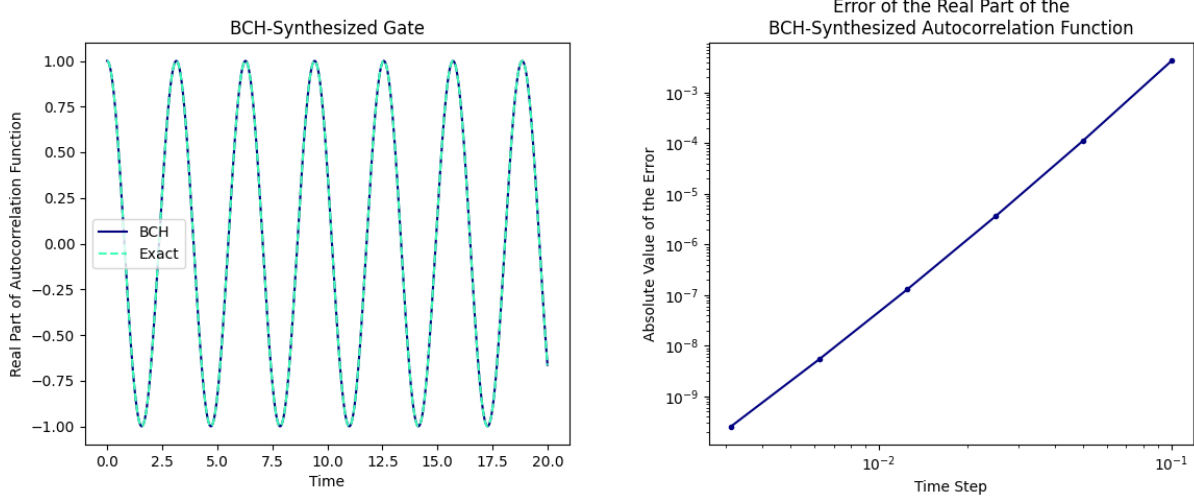


Figure 1: The following plots characterize the performance of using phase-space operators to synthesize  $e^{i\hat{n}\sigma^z t}$ . (a) The BCH-synthesized conditional rotation gate  $e^{i\hat{n}\sigma^z t}$  successfully reproduces the exact dynamics for a wavefunction initialized in the ground state of the transmon and the second excited state of the cavity. (b) Error of the real part of the autocorrelation function for the BCH-synthesized gate after a single time step of length  $t$ .

To begin, we recognize that we intuitively aim to implement  $(a^\dagger)^k$  on the vacuum. It is sufficient to approximate:

$$\mathcal{T}_k(t) := \exp it \begin{bmatrix} 0 & (a^\dagger)^k \\ a^k & 0 \end{bmatrix}. \quad (65)$$

Because selecting appropriate  $t$  yields precisely the desired behavior, we have the following result:

**Theorem D.5.** *For  $k \leq \Lambda$ , we can take  $t = (2n + 1)\frac{\pi}{2\sqrt{k!}}$  for any  $n \in \mathbb{N}$  so that:*

$$\mathcal{T}_k(t) |1\rangle \otimes |0\rangle = |0\rangle \otimes |k\rangle.$$

Note here that we can implement such a mapping using the Baker-Campbell-Hausdorff formula (BCH).

While  $\mathcal{T}_k(t)$  performs the desired transformation, it may incur unwanted side effects if the starting state is of the form  $|1\rangle \otimes |b\rangle$  for  $b > 0$ . We can use our same approach to produce the following operation:

**Theorem D.6.** *Consider the Fock preparation unitary  $\mathcal{P}_k$  with the following form:*

$$\exp \left( it \begin{bmatrix} 0 & (a^\dagger)^k |0\rangle\langle 0| \\ |0\rangle\langle 0| (a)^k & 0 \end{bmatrix} \right).$$

When  $t = (2n + 1)\frac{\pi}{4\sqrt{k!}}$ , we have that  $\mathcal{P}_k$  performs our desired state preparation:

$$\exp \left( it \begin{bmatrix} 0 & (a^\dagger)^k |0\rangle\langle 0| \\ |0\rangle\langle 0| (a)^k & 0 \end{bmatrix} \right) |1\rangle \otimes |b\rangle = \begin{cases} |0\rangle \otimes |k\rangle & b = 0 \\ |1\rangle \otimes |b\rangle & b \neq 0 \end{cases}.$$

We claim that we can approximate this unitary with  $\tilde{\mathcal{P}}_{k,p}$  where:

$$\left\| \tilde{\mathcal{P}}_{k,p} - \mathcal{P}_k \right\| \in \mathcal{O}((\Lambda^{k/2}t)^p),$$

using no more than  $4 \cdot 5^{q-1} \tilde{\mathcal{T}}_{k,p}$  subroutines.

Where the proofs are provided in [Appendix D.3](#). Though this subroutine appears expensive, numerical results suggest it is far more implementable than theory would suggest. In the following simulations, we apply the above technique but always use a second-order symmetrized BCH formula and second-order (symmetrized) Trotter formula. This amounts to 480 exponentials for the unprotected case and 960 exponentials for the protected case. The error plot is provided in [Figure 2](#) and [Figure 3](#).

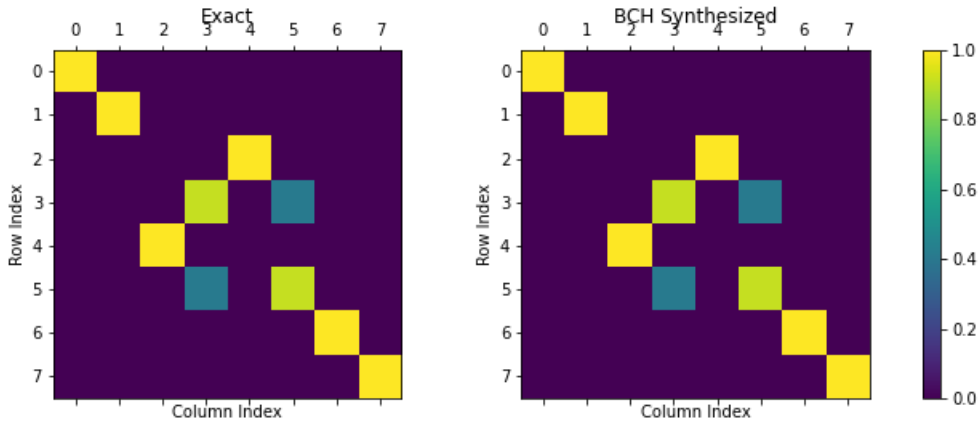


Figure 2: Unprotected  $T_2$  Gate: (a) is the exact form of the  $T_2$  gate with selected  $t$  and (b) is the BCH-synthesized form. The state  $|j\rangle_q |k\rangle_m$  has index  $j \cdot \Lambda + k$  where  $\Lambda$  is the cutoff. By observation, the analytically realized form is accurate.

We also analyze the error scaling as the order of the BCH formulas used increases. [Figure 4](#) describes the error-resource tradeoff as the Trotter step within each BCH formula increases.

#### 4.4 Hong-Ou-Mandel effect/conditional (controlled-phase) beam splitter gate

The operations we seek to realize need not act on a single mode; in fact, our techniques are extensible to hybrid setups with multiple modes or qubits. Consider the conditional (controlled-phase) beam splitter

$$U_{\text{beam split}} = e^{-i\lambda^2 (\hat{a}_1^\dagger \hat{a}_2 + \hat{a}_1 \hat{a}_2^\dagger) \sigma^z}. \quad (66)$$

This gate naturally pertains to certain lattice gauge theories and gives rise to exponential SWAP (eSWAP) [\[30\]](#) and controlled-SWAP (cSWAP) gates for state purification and SWAP tests, when paired with an uncontrolled beam splitter [\[31\]](#). The argument in phase-space representation is

$$-i\lambda^2 (\hat{a}_1^\dagger \hat{a}_2 + \hat{a}_1 \hat{a}_2^\dagger) \sigma^z = -2i\lambda^2 (\hat{x}_1 \hat{x}_2 + \hat{p}_1 \hat{p}_2) \sigma^z, \quad (67)$$



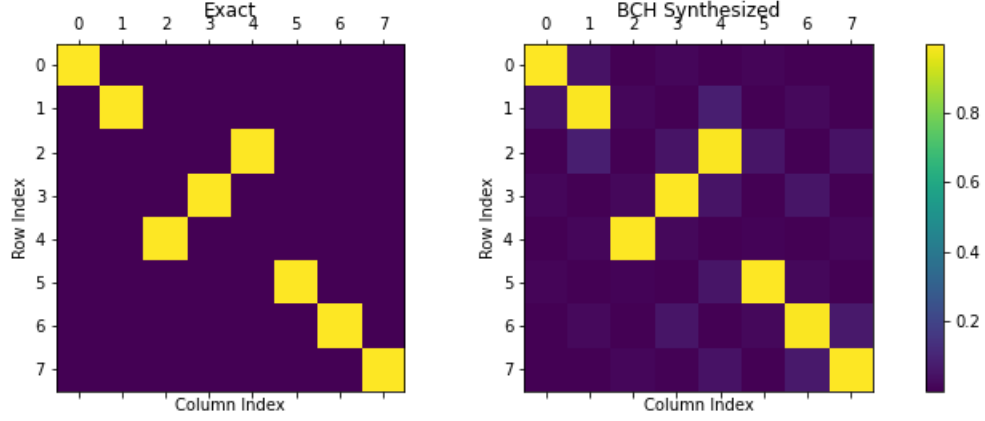


Figure 3: Protected  $T_2$  Gate: (a) is the exact form of the protected  $T_2$  gate with selected  $t$  and (b) is the BCH-synthesized form. The state  $|j\rangle_q |k\rangle_m$  has index  $j \cdot \Lambda + k$  where  $\Lambda$  is the cutoff. By observation, the analytically realized form is still accurate, albeit with more incurred Trotter error.

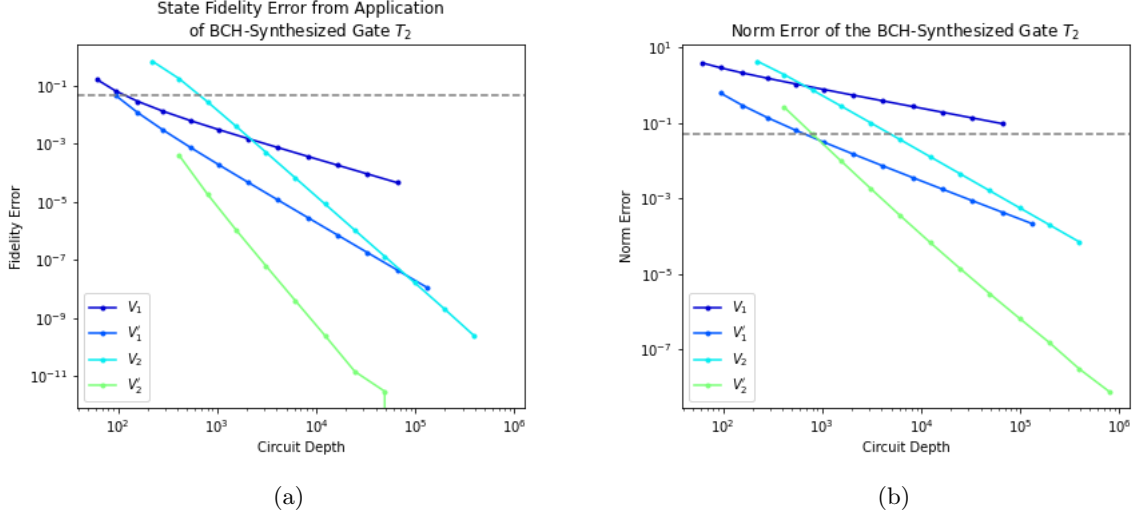


Figure 4: Error scaling of protected  $T_2$  gate with respect to BCH circuit depth. Prime denotes that the formula has been symmetrized. (a) uses the state-fidelity metric while (b) uses the matrix norm.

such that the gate is decomposed in terms of a Trotter-Suzuki expansion as the product of two exponential terms  $\exp([A_1, B_1] \lambda^2) = \exp(-2i\lambda^2 \hat{x}_1 \hat{x}_2 \sigma^z)$  and  $\exp([A_2, B_2] \lambda^2) = \exp(-2i\lambda^2 \hat{x}_1 \hat{x}_2 \sigma^z)$ . According to the Pauli commutation relation the first commutator is

$$[A_1, B_1] = -2i\hat{x}_1 \hat{x}_2 \sigma^z \quad (68)$$

$$= -2i\hat{x}_1 \hat{x}_2 \left( -\frac{i}{2} [\sigma^x, \sigma^y] \right) \quad (69)$$

$$= [i\hat{x}_1 \sigma^x, i\hat{x}_2 \sigma^y], \quad (70)$$

and the second is

$$[A_2, B_2] = [i\hat{p}_1\sigma^x, i\hat{p}_2\sigma^y], \quad (71)$$

with the following error scaling:

**Theorem C.2.** *Assume we may implement  $e^{it\hat{x}_m\sigma^j}$ ,  $e^{it\hat{p}_m\sigma^j}$  for  $m \in \{1, 2\}$ ; i.e., we may implement the qubit-conditional position shifts and momentum boosts on either mode without error. Then, we may approximate  $\mathcal{B}_{\hat{x}_1\hat{x}_2+\hat{p}_1\hat{p}_2}$  with arbitrary error scaling  $p$ :*

$$\left\| \tilde{\mathcal{B}}_{\hat{x}_1\hat{x}_2+\hat{p}_1\hat{p}_2} - \mathcal{B}_{\hat{x}_1\hat{x}_2+\hat{p}_1\hat{p}_2} \right\| \in \mathcal{O}((Ct)^{p+\frac{1}{2}}),$$

where  $C = \max(\|\hat{x}_1\hat{x}_2 + \hat{p}_1\hat{p}_2\|, \|\hat{x}_1\|^2, \|\hat{x}_2\|^2, \|\hat{p}_1\|^2, \|\hat{p}_2\|^2)$  and using no more than  $4 \cdot 5^{\frac{p}{2}-\frac{1}{4}}$  exponentials.

The two exponential terms are decomposed via the BCH formula for a lower-bound gate depth of eight. Results are shown in Fig. 5 for 15 states per cavity with a shared transmon over a final time of  $\pi/2$  with 200 equal time steps, where the system is initially in the first excited state of each cavity and the ground state of the shared transmon  $|11g\rangle$ . As expected for the conditional beam splitter, the gate exhibits the Hong-Ou-Mandel effect, in which the occupation of cavity 1 oscillates between the first excited mode and a superposition of the ground and the second excited states of the cavity. The BCH-synthesized results closely agree with that of the original gate, with no visible leakage beyond the physical states (the lowest three states of the cavity) into the working space under the time duration studied. As for the conditional rotation gate, the relative error of the BCH-synthesized gate computed for a single time step of length  $t$  was found to scale according to a power law with the time step, in accordance with the analytic result for Trotterization and BCH decomposition.

## 5 Discussion

Our main contribution in this paper is a systematic approach to synthesizing unitary dynamics on a hybrid quantum computer that has access to both qubit as well as bosonic operations. Such gatesets naturally model systems such as cavity quantum electrodynamics systems as well as ion trap-based quantum computers. Our main innovation here is the development of high-order analytic formulas that can be used to place bounds on the complexity of implementing arbitrary unitary operations on such a hybrid device. Specifically, we see that these methods are capable of achieving subpolynomial scaling with the inverse error tolerance ( $1/\epsilon$ ) and allows us to implement arbitrary nonlinearities in the field operators in the generator of the unitary that we wish to implement at low cost asymptotically. In particular, we focus on using a construct known as a block-encoded creation operator as our fundamental construct and show numerically highly accurate approximations to the exponential of a block-encoding of the square of the creation operator. Further, we study the Hong-Ou-Mandel effect and observe that the synthesized operations used in our construction can have negligible error with respect to our target precision.

While this work constitutes a significant step forward in our understanding of how to control and manipulate such quantum systems, there remain many open questions. The first issue involves the large constant-factor overheads observed in practical implementations of our synthesized operations within this gate set. Specifically, we note that for both the Hong-Ou-Mandel effect and the block-encoding of  $(a^\dagger)^2$  that thousands of gate operations are needed to achieve infidelities of  $10^{-3}$  or smaller. This makes such sequences impractical for near-term applications where the gate infidelities

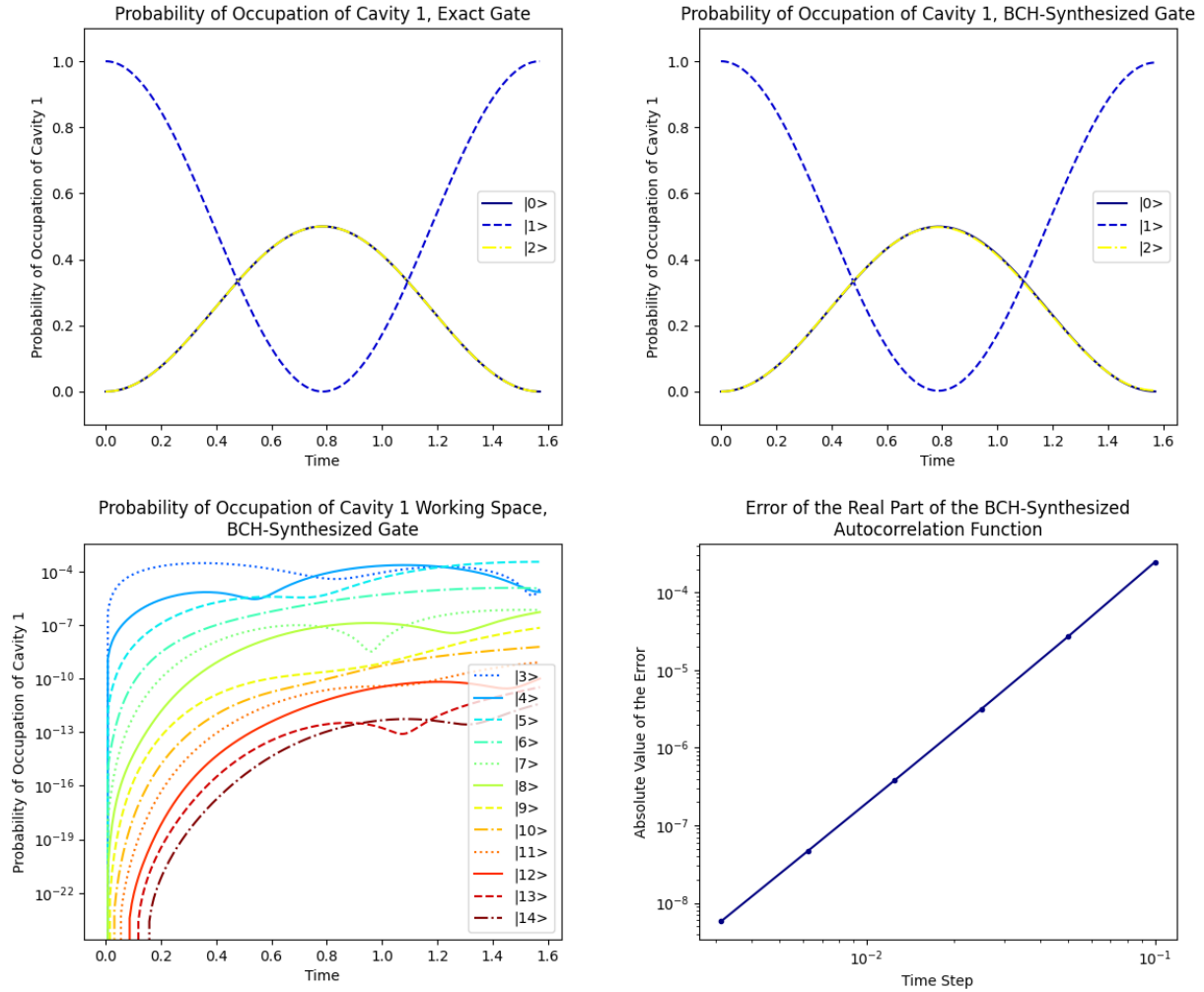


Figure 5: Hong-Ou-Mandel effect simulated with (a) exact and (b) BCH-synthesized conditional beam splitters, illustrated as probability cavity 1 is found in states  $|0\rangle$ ,  $|1\rangle$ , or  $|2\rangle$ ; (c) probability of leakage into higher cavity modes; and (d) error of the real part of the autocorrelation after a single application of a BCH-synthesized gate for time step  $t$  relative to the application of the exact gate for the same time step.

are on the order of 1%. Several avenues of approach exist that could be used to improve upon these results. The first approach would be to use ideas related to quantum signal processing to implement functions of creation operators; this could potentially improve the scaling with respect to the error tolerance from the subpolynomial scaling currently demonstrated to polylogarithmic scaling. The second approach would be to use sequences designed here as seeds for gradient-descent optimization procedures for control such as GRAPE [13] at the pulse level or numerical optimization of parameterized gates at the SNAP [32] or Controlled Displacement [17] instruction level. These locally optimized sequences may then prove to be either better, or more understandable, than existing gradient-optimized pulse sequences for control of such systems.

## Acknowledgements

This project was primarily supported by the U.S. Department of Energy, Office of Science, National Quantum Information Science Research Centers, Co-design Center for Quantum Advantage under contract number DE-SC0012704, (Basic Energy Sciences, PNNL FWP 76274). Eleanor Crane was supported by UCL Faculty of Engineering Sciences and the Yale-UCL exchange scholarship from RIGE (Research, Innovation and Global Engagement), and by the Princeton MURI award SUB0000082, the DoE QSA, NSF QLCI (award No.OMA-2120757), DoE ASCR Accelerated Research in Quantum Computing program (award No.DESC0020312), NSF PFCQC program. Micheline B. Soley was supported by the Yale Quantum Institute Postdoctoral Fellowship.

## APPENDICES

### A Obtaining $S_1$

Here, we demonstrate how to obtain the  $S_1$  operator, with the native gates present in the dispersive coupling regime.

The controlled displacement operator with magnitude  $\alpha$  is written:

$$U_d(\alpha) = e^{i(\alpha a^\dagger + \alpha^* a) \otimes \sigma^z}. \quad (72)$$

For a Fock state  $|n\rangle$ ,  $a^\dagger a |n\rangle = n |n\rangle$ ; therefore  $e^{ia^\dagger a \theta} a^\dagger e^{-ia^\dagger a \theta} = e^{i\theta} a^\dagger$ . Taking  $\alpha = \alpha^*$ , we have

$$e^{i(\pi/2)a^\dagger a} e^{i(\alpha(a^\dagger + a)) \otimes \sigma^y} e^{-i(\pi/2)a^\dagger a} = \exp \left( \alpha \begin{bmatrix} 0 & (ia^\dagger - ia) \\ (-ia^\dagger + ia) & 0 \end{bmatrix} \right). \quad (73)$$

This operation can be built using single-qubit operations on a controlled displacement gate with additional phase delays on the oscillator. Both are linear optical operations or single-qubit operations, which we expect to be inexpensive in our computational model.

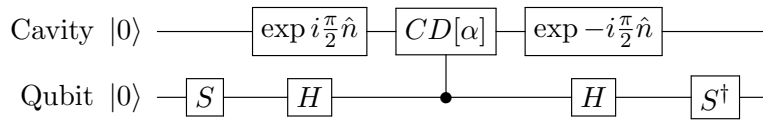
Next, note that

$$e^{i(\alpha(a^\dagger + a)) \otimes \sigma^x} = \exp \left( \alpha \begin{bmatrix} 0 & i(a^\dagger + a) \\ i(a^\dagger + a) & 0 \end{bmatrix} \right). \quad (74)$$

Thus to  $O(\alpha^2)$  the block-encoded creation operation can be constructed using single-qubit operations, two controlled displacement operations and linear optical operations through

$$S_1 \approx e^{i(\pi/2)a^\dagger a} e^{i(\alpha(a^\dagger + a)) \otimes \sigma^y} e^{-i(\pi/2)a^\dagger a} e^{i(\alpha(a^\dagger + a)) \otimes \sigma^x}. \quad (75)$$

This provides an intuition for our strategy for compiling gates. A major goal in this work is to optimize such formulas to minimize the number of operations needed to closely approximate evolution. To this end, symmetric and higher-order approximations of this form will be vital to achieving the optimal scaling for such formulas and in turn get a deeper understanding of the costs of hybrid boson-qubit computations.



### B Error analysis

To assess the error scaling of the addition algorithm, we must consider three sources of error: the underlying implementation error from using approximations of  $\mathcal{B}_A(t)$ , the error from BCH, and the error from Trotter. In [Appendix B.1](#), we show that the BCH and Trotter formulas can still be applied on exponentials that have error. Then, we use these formulas in [Appendix B.2](#) to produce the error bounds for addition. Finally, in [Appendix B.3](#), we produce the error bounds for multiplication.

## B.1 Product formulas with implementation error

We begin by formally stating the Trotter and BCH formulas when there is no implementation error:

**Theorem B.1** (BCH Product Formula (Theorem 2 from [25])). *Let  $A$  and  $B$  be bounded complex-valued matrices and assume without loss of generality  $t \in \mathbb{R}^+$  is assumed for the purposes of asymptotic analysis to be in  $o(1)$ . We then define*

$$\text{BCH}_{1,k}(At, Bt^k) := e^{At} e^{Bt^k} e^{-At} e^{-Bt^k}. \quad (76)$$

We further define  $\text{BCH}_{p,k}$  recursively for  $p \geq 2$  and odd  $k \geq 1$ :

$$\text{BCH}_{p+1,k}(At, Bt^k) := \text{BCH}_{p,k}(A\gamma_p t, B(\gamma_p t)^k) \text{BCH}_{p,k}(-A\gamma_p t, -B(\gamma_p t)^k) \quad (77)$$

$$\times \text{BCH}_{p,k}(A\beta_p t, B(\beta_p t)^k)^{-1} \text{BCH}_{p,k}(-A\beta_p t, -B(\beta_p t)^k)^{-1} \quad (78)$$

$$\times \text{BCH}_{p,k}(A\gamma_p t, B(\gamma_p t)^k) \text{BCH}_{p,k}(-A\gamma_p t, -B(\gamma_p t)^k), \quad (79)$$

with the following constants:

$$\beta_p := (2r_p)^{1/(k+1)}, \gamma_p := (1/4 + r_p)^{1/(k+1)}, r_p := \frac{2^{\frac{(k+1)}{2p+k+1}}}{4 \left(2 - 2^{\frac{k+1}{2p+k+1}}\right)}. \quad (80)$$

This recursive formula has the following error scaling, where  $\gamma = \max(\|A\|, \|B\|^{1/k})$  [25]:

$$\text{BCH}_{p,k}(At, Bt^k) = e^{[A,B]t^{k+1} + \mathcal{O}((\gamma t)^{2p+k})} \quad (81)$$

and uses  $8 \cdot 6^{p-1}$  exponentials when  $k = 1$  and  $4 \cdot 6^{p-1}$  exponentials otherwise.

**Theorem B.2** (Trotter Formula (Lemma 1 from [23])). *Let  $\{H_j : j = 1 \dots m\}$  be a set of  $M$  bounded Hermitian operators acting on a Hilbert space of dimension  $2^n$  and assume without loss of generality that  $t \geq 0$ . For  $H = \sum H_j$ , the error in the Trotter-Suzuki formulas of order  $k$  and timestep  $r$  obeys the following error bound:*

$$\left\| \exp\left(-it \sum_{j=1}^m H_j\right) - \text{Trotter}_{2k}(\{H_j\}, t/r)^r \right\| \leq 5(2 \times 5^{k-1} m \tau)^{2k+1} / r^{2k}, \quad (82)$$

where  $\tau = \|H\| t$  and

$$4m5^{k-1}\tau/r \leq 1, \quad (83)$$

$$(16/3)(2 \times 5^{k-1} m \tau)^{2k+1} / r^{2k} \leq 1, \quad (84)$$

using no more than  $2m5^{k-1}r$  exponentials. We define the  $k^{\text{th}}$  order Trotter formula as:

$$\text{Trotter}_{2k}(\lambda) := [\text{Trotter}_{2k-2}(p_k \lambda)]^2 \text{Trotter}_{2k-2}((1 - 4p_k)\lambda) [\text{Trotter}_{2k-2}(p_k \lambda)]^2,$$

where  $p_k = (4 - 4^{1/(2k-1)})^{-1}$  and  $k > 1$ . The relation has the following base case:

$$\text{Trotter}_2(\lambda) = \prod_{j=1}^m e^{H_j \lambda/2} \prod_{j'=m}^1 e^{H_{j'} \lambda/2},$$

which implies the following corollary:

**Corollary B.1.** *If  $r = 1$ , i.e. there is no time stepping, the Trotter formula exhibits the following error scaling:*

$$\left\| \exp \left( -it \sum_{j=1}^m H_j \right) - \text{Trotter}_{2k}(\{H_j\}, t) \right\| \in \mathcal{O}(\|H\| t^{2k+1}), \quad (85)$$

using no more than  $2m5^{k-1}$  exponentials.

Both of these formulas, however, assume that our implementation of exponentials occurs without error. However, if we would like to apply our technique recursively, our matrix product formulas must account for implementation error, i.e. be able to use primitives that themselves may have error. Thus, we restate both Trotter and BCH when the operators have asymptotic error:

**Lemma B.1** (BCH under implementation error). *Suppose there are some ideal operators  $U_1(t), U_2(t)$  which are exponentials of some anti-Hermitian matrix, i.e.:*

$$U_1(t) = \exp tA_1, \quad (86)$$

$$U_2(t) = \exp tA_2. \quad (87)$$

We seek to build  $\exp t^2[A_1, A_2]$ , the exponential of the commutator of the matrices. Also suppose that may approximate  $U_1(t), U_2(t)$  with  $\tilde{U}_{1,p_1}(t), \tilde{U}_{2,p_2}(t)$  with the following error scaling:

$$\left\| \tilde{U}_{1,p_1}(t) - U_1(t) \right\| \in \mathcal{O}((ct)^{p_1}), \quad (88)$$

$$\left\| \tilde{U}_{2,p_2}(t) - U_2(t) \right\| \in \mathcal{O}((ct)^{p_2}), \quad (89)$$

for some  $p_1, p_2 \geq 1$ . Then, applying a  $q^{\text{th}}$ -ordered BCH formula, where  $q = \max(\lceil \frac{\min(p_1, p_2) - 1}{2} \rceil, 1)$  on the implementable  $\tilde{U}_{1,p_1}(t), \tilde{U}_{2,p_2}(t)$  can still approximate the commutator exponential by applying [Theorem B.1](#):

$$\left\| \exp t^2[A_1, A_2] - \text{BCH}_{q,r}(\tilde{U}_{1,p_1}(t), \tilde{U}_{2,p_2}(t)) \right\| \in \mathcal{O}((Ct)^{\min(p_1, p_2)}), \quad (90)$$

where  $C = \max(\|A_1\|, \|A_2\|, c)$ . This procedure uses  $8 \cdot 6^{q-1}$  total exponentials.

*Proof.* Recognize that we may decompose the error involved in implementing the commutator exponential into two sources: the error incurred from the BCH formula intrinsically and the implementation error from the realizable terms. Thus, by the triangle inequality:

$$\begin{aligned} & \left\| \exp t^2[A_1, A_2] - \text{BCH}_q(\tilde{U}_{1,p_1}(t), \tilde{U}_{2,p_2}(t)) \right\| \leq \\ & \left\| \exp t^2[A_1, A_2] - \text{BCH}_q(U_1(t), U_2(t)) \right\| + \left\| \text{BCH}_q(U_1(t), U_2(t)) - \text{BCH}_q(\tilde{U}_{1,p_1}(t), \tilde{U}_{2,p_2}(t)) \right\|. \end{aligned} \quad (91)$$

We begin with the LHS term. By [Theorem B.1](#),

$$\left\| \exp t^2[A_1, A_2] - \text{BCH}_q(U_1(t), U_2(t)) \right\| \in \mathcal{O}(C_{\text{BCH}} t^{2q+1}), \quad (92)$$

where  $C_{\text{BCH}} = \max(\|A_1\|, \|A_2\|)$ . For the RHS, recall by Box 4.1 of Nielsen and Chuang [\[33\]](#) that implementation errors accumulate at most linearly; thus, we can sum over the  $8 \cdot 6^{q-1}$  operations used

by BCH. By symmetry of the BCH formula, we apply the  $\tilde{U}_{1,p_1}(t), \tilde{U}_{2,p_2}(t)$  exponentials precisely  $4 \cdot 6^{q-1}$  times. Thus:

$$\left\| \text{BCH}_q(U_1(t), U_2(t)) - \text{BCH}_q(\tilde{U}_{1,p_1}(t), \tilde{U}_{2,p_2}(t)) \right\| \leq \sum_{j=1}^{4 \cdot 6^{q-1}} \mathcal{O}((ct)^{p_1}) + \mathcal{O}((ct)^{p_2}) \quad (93)$$

$$\in \mathcal{O}((ct)^{\min(p_1, p_2)}). \quad (94)$$

Setting  $q = \max\{\lceil \frac{\min(p_1, p_2) - 1}{2} \rceil, 1\}$  and recalling  $\gamma \geq 1$ , observe:

$$\left\| \exp t^2[A_1, A_2] - \text{BCH}_q(\tilde{U}_{1,p_1}(t), \tilde{U}_{2,p_2}(t)) \right\| \in \mathcal{O}((Ct)^{\min(p_1, p_2)}), \quad (95)$$

as desired.  $\square$

**Lemma B.2** (Trotter under implementation error). *Given Lemma B.1's assumptions, Theorem B.2's assumptions, and assuming  $\|A_1 + A_2\| \geq 1$ , an operator can be constructed by applying a  $q^{\text{th}}$ -ordered Trotter formula  $\text{Trotter}_{2q}$  by setting  $q = \max(\lceil \frac{\min(p_1, p_2) - 1}{2} \rceil, 1)$  so that:*

$$\left\| \exp t(A_1 + A_2) - \text{Trotter}_q(\tilde{U}_{1,p_1}(t), \tilde{U}_{2,p_2}(t)) \right\| \in \mathcal{O}((Ct)^{\min(p_1, p_2)}), \quad (96)$$

where  $C = \max(\|A_1 + A_2\|, c)$  and using no more than  $4 \cdot 5^{q-1}$  operator exponentials.

*Proof.* Similarly, we may apply the triangle inequality in order to determine a bound by separating the error accrued into the intrinsic Trotter error and the implementation error:

$$\begin{aligned} & \left\| \exp t(A_1 + A_2) - \text{Trotter}_{2q}(\tilde{U}_{1,p_1}(t), \tilde{U}_{2,p_2}(t)) \right\| \\ & \leq \left\| \exp t(A_1 + A_2) - \text{Trotter}_{2q}(U_1(t), U_2(t)) \right\| \\ & \quad + \left\| \text{Trotter}_{2q}(U_1(t), U_2(t)) - \text{Trotter}_{2q}(\tilde{U}_{1,p_1}(t), \tilde{U}_{2,p_2}(t)) \right\|. \end{aligned} \quad (97)$$

To analyze the LHS, which represents the Trotter error, Corollary B.1 provides a bound:

$$\left\| \exp t(A_1 + A_2) - \text{Trotter}_{2q}(U_1(t), U_2(t)) \right\| \in \mathcal{O}(\|A_1 + A_2\| t^{2q+1}). \quad (98)$$

For the RHS, which represents the implementation error, recall by box 4.1 of Nielsen and Chuang [33] that the error accrues linearly. Furthermore, the number of operations in Trotter is no more than  $4 \cdot 5^{q-1}$  operations in total. Therefore, we only apply each constituent operation at most  $2 \cdot 5^{q-1}$  times. Thus, a loose upper bound can be written as:

$$\left\| \text{Trotter}_{2q}(U_1(t), U_2(t)) - \text{Trotter}_{2q}(\tilde{U}_{1,p_1}(t), \tilde{U}_{2,p_2}(t)) \right\| \leq \sum_{j=1}^{4 \cdot 5^{q-1}} \mathcal{O}((ct)^{p_1}) + \mathcal{O}((ct)^{p_2}) \quad (99)$$

$$\in \mathcal{O}((ct)^{\min(p_1, p_2)}). \quad (100)$$

It is sufficient to set  $q = \max(\lceil \frac{\min(p_1, p_2) - 1}{2} \rceil, 1)$  so that:

$$\left\| \exp t(A_1 + A_2) - \text{Trotter}_{2q}(\tilde{U}_{1,p_1}(t), \tilde{U}_{2,p_2}(t)) \right\| \quad (101)$$

$$\in \mathcal{O}(\|A_1 + A_2\| t^{2q+1}) + \mathcal{O}((ct)^{\min(p_1, p_2)}) = \mathcal{O}((Ct)^{\min(p_1, p_2)}), \quad (102)$$

as desired.  $\square$



## B.2 Scaling of the addition algorithm

We apply the above results to produce the error analysis of [Algorithm 1](#):

**Theorem 3.1.** *Suppose we have approximations  $\tilde{\mathcal{B}}_A(t), \tilde{\mathcal{B}}_B(t)$  with the following error scaling:*

$$\left\| \tilde{\mathcal{B}}_A(t) - \mathcal{B}_A(t) \right\| \in \mathcal{O}((ct)^{p_A}), \quad (44)$$

$$\left\| \tilde{\mathcal{B}}_B(t) - \mathcal{B}_B(t) \right\| \in \mathcal{O}((ct)^{p_B}), \quad (45)$$

for some constant  $c$  and order  $p_A, p_B \geq 1$  where  $[A, B] = 0$ . Then, the application of [Algorithm 1](#) will yield the following scaling:

$$\left\| \text{ADD}(\tilde{\mathcal{B}}_A(t), \tilde{\mathcal{B}}_B(t)) - \exp it \begin{bmatrix} 0 & AB \\ BA & 0 \end{bmatrix} \right\| \in \mathcal{O}\left((C_{TOTAL}t)^{\min(p_A, p_B)/2}\right), \quad (46)$$

with  $C_{TOTAL} = \max(\|AB\|, \|BA\|, C_{BCH}^2)$  and  $C_{BCH} = \max(\|A\|, \|B\|, c)$ , using no more than  $1.07 \cdot 30^q$  exponentials, where  $q = \max(\lceil \frac{\min(p_1, p_2) - 1}{2} \rceil, 1)$ .

*Proof.* Our proof proceeds by applying the above theorems upon our operations. By setting  $q = \max(\lceil \frac{\min(p_1, p_2) - 1}{2} \rceil, 1)$ , [Lemma B.1](#) implies that:

$$\left\| \text{BCH}_q(X\tilde{\mathcal{B}}_B(\tau)X, \tilde{\mathcal{B}}_A(\tau)) - \exp \tau^2[A, B]\sigma^z \right\| \in \mathcal{O}((C_{BCH}\tau)^{p_{BCH}}), \quad (103)$$

$$\left\| \text{BCH}_q(S\tilde{\mathcal{B}}_A(\tau)S^\dagger, X\tilde{\mathcal{B}}_B(\tau)X) - \exp i\tau^2\{A, B\}\sigma^z \right\| \in \mathcal{O}((C_{BCH}\tau)^{p_{BCH}}), \quad (104)$$

where  $C_{BCH} = \max(\|A\|, \|B\|, c)$  and  $p_{BCH} = \min(p_A, p_B)$ . We'll need to set  $\tau = \sqrt{\frac{t}{2}}$  to achieve the desired time evolution. Additionally, Pauli conjugation has no impact on the error scaling. Call these formulas ‘‘Left’’ and ‘‘Right’’:

$$\text{LEFT} := SH \cdot \text{BCH}_q(X\tilde{\mathcal{B}}_B(\tau)X, \tilde{\mathcal{B}}_A(\tau)) \cdot HS^\dagger, \quad (105)$$

$$\text{RIGHT} := HB\text{BCH}_q(S\tilde{\mathcal{B}}_A(\tau)S^\dagger, X\tilde{\mathcal{B}}_B(\tau)X)H, \quad (106)$$

where:

$$\left\| \text{LEFT} - \exp \tau^2(AB - (AB)^\dagger)\sigma^y \right\| \in \mathcal{O}((C^2t)^{p_{BCH}/2}), \quad (107)$$

$$\left\| \text{RIGHT} - \exp i\tau^2(AB + (AB)^\dagger)\sigma^x \right\| \in \mathcal{O}((C^2t)^{p_{BCH}/2}). \quad (108)$$

Finally, we use [Lemma B.2](#), implying that a Trotter formula with order  $q$  has the following error scaling:

$$\left\| \text{Trotter}_s(\text{LEFT}, \text{RIGHT}) - \exp it \begin{bmatrix} 0 & (AB)^\dagger \\ AB & 0 \end{bmatrix} \right\| \in \mathcal{O}((C_{TOTAL}t)^{p_{BCH}/2}), \quad (109)$$

where:

$$C_{TOTAL} = \max\left(\left\| \begin{bmatrix} 0 & (AB)^\dagger \\ AB & 0 \end{bmatrix} \right\|, C_{BCH}^2\right) = \max\left(\|AB\|, \|(AB)^\dagger\|, C_{BCH}^2\right). \quad (110)$$

To bound the number of operations used, recognize that the Trotter formula requires at most  $4 \cdot 5^{q-1}$  commutators, each of which requires  $8 \cdot 6^{q-1}$  constituent operators. Thus, the total number of operators required is bounded as follows:

$$4 \cdot 5^{q-1} \cdot 8 \cdot 6^{q-1} \leq 1.07 \cdot 30^q, \quad (111)$$

□

which implies the following corollary for the annihilation/creation operators:

**Corollary B.2** (Algorithm 1 applied to polynomials of annihilation/creation operators). *Assume we can implement the following  $k_l, k_r^{\text{th}}$  order approximations of  $S$  with error scaling  $p_l, p_r$ :*

$$\left\| \tilde{\mathcal{S}}_{k_l, p_l}(t) - \mathcal{S}_{k_l}(t) \right\| \in \mathcal{O}((ct)^{p_l}), \quad (112)$$

$$\left\| \tilde{\mathcal{S}}_{k_r, p_r}(t) - \mathcal{S}_{k_r}(t) \right\| \in \mathcal{O}((ct)^{p_r}), \quad (113)$$

with  $c \geq \Lambda^{\max(k_l, k_r)/2}$ . Then, we can implement higher order operators with comparable  $t$  scaling:

$$\left\| \tilde{\mathcal{S}}_{k_l+k_r, \min(p_l, p_r)}(t) - \exp \left( it \begin{bmatrix} 0 & (a^\dagger)^{k_l+k_r} \\ a^{k_l+k_r} & 0 \end{bmatrix} \right) \right\| \in \mathcal{O}((c^2t)^{\min(p_l, p_r)/2}), \quad (114)$$

using no more than  $1.07 \cdot 30^q$   $\mathcal{S}_{k_l}, \mathcal{S}_{k_r}$  operators.

*Proof.* To synthesize the block-encoding of higher-order annihilation/creation operators, we will directly apply Theorem 3.1. We quantify the error by bounding the block-encoding norm. Note that:

**Fact B.3.** *A  $k^{\text{th}}$  order block-encoded operator has a bounded norm:*

$$\left\| \begin{bmatrix} 0 & (a^\dagger)^k \\ (a)^k & 0 \end{bmatrix} \right\| \leq \Lambda^{k/2}. \quad (115)$$

Thus, the constant  $C_{\text{BCH}}$  is bounded, as  $C_{\text{BCH}} \leq \max(\Lambda^{k_l/2}, \Lambda^{k_r/2}, c) \leq \max(\Lambda^{\max(k_l, k_r)/2}, c) = c$  by hypothesis. Next, observe that  $\|AB\|, \|(AB)^\dagger\| \leq \Lambda^{(k_l+k_r)/2}$ . Thus,  $C_{\text{TOTAL}} \leq \max(\Lambda^{(k_l+k_r)/2}, c^2) = c^2$ . Therefore, the final error scaling will be upper bounded by  $\mathcal{O}((c^2t)^{\min(p_l, p_r)/2})$ .  $\square$

### B.3 Scaling of the multiplication algorithm

Algorithm 2's error scaling follows directly from the BCH formula:

**Theorem 3.2.** *Suppose we have some approximate block encodings  $\tilde{\mathcal{B}}_A, \tilde{\mathcal{B}}_B$  with the following error:*

$$\left\| \tilde{\mathcal{B}}_A(t) - \exp it \begin{bmatrix} 0 & A \\ A^\dagger & 0 \end{bmatrix} \right\| \in \mathcal{O}((ct)^{p_A}), \quad (47)$$

$$\left\| \tilde{\mathcal{B}}_B(t) - \exp it \begin{bmatrix} 0 & B \\ B^\dagger & 0 \end{bmatrix} \right\| \in \mathcal{O}((ct)^{p_B}), \quad (48)$$

for constant  $c$  and  $p_A, p_B \geq 1$  where  $AB = (AB)^\dagger$ . Then, Algorithm 2 has the following error:

$$\left\| \text{MULT}(\tilde{\mathcal{B}}_A(t), \tilde{\mathcal{B}}_B(t)) - \exp it \begin{bmatrix} AB & 0 \\ 0 & \frac{1}{2}(-BA - (BA)^\dagger) \end{bmatrix} \right\| \in \mathcal{O} \left( (C^2t)^{\min(p_A, p_B)/2} \right), \quad (49)$$

with  $C = \max(\|A\|, \|B\|, c)$ , using no more than  $8 \cdot 6^{q-1}$  exponentials where  $q = \max(\lceil \frac{\min(p_A, p_B)-1}{2} \rceil, 1)$ .

*Proof.* We can directly apply Lemma B.1 using the  $\tilde{\mathcal{B}}_A, \tilde{\mathcal{B}}_B$  operators. When applied, we find that:

$$\left\| \text{BCH}_q(S\tilde{\mathcal{B}}_A(\tau)S^\dagger, \tilde{\mathcal{B}}_B(\tau)) - \exp 2i\tau^2 \begin{bmatrix} AB & 0 \\ 0 & -BA - (BA)^\dagger \end{bmatrix} \right\| \in \mathcal{O}((C\tau)^{\min(p_A, p_B)}), \quad (116)$$

where  $C = \max(\|A\|, \|B\|, c)$  and  $q = \max(\lceil \frac{\min(p_A, p_B) - 1}{2} \rceil, 1)$ . Then, by taking  $\tau = \sqrt{\frac{t}{2}}$ , we yield:

$$\left\| \text{BCH}_q(S\tilde{\mathcal{B}}_B(\tau)S^\dagger, \tilde{\mathcal{B}}_A(\tau)) - \exp it \begin{bmatrix} AB & 0 \\ 0 & -BA \end{bmatrix} \right\| \in \mathcal{O}((C\tau)^{\min(p_A, p_B)}) = \mathcal{O}((C^2t)^{\min(p_A, p_B)/2}). \quad (117)$$

By counting the number of exponentials in the result via [Lemma B.1](#) we finally find that the number of exponentials needed is at most  $8 \cdot 6^{q-1}$ .  $\square$

## C Phase-Space Applications

In the following section, we derive error bounds for the two phase-space applications described: the conditional rotation gate and the controlled-phase beam splitter. However, the typical cutoff approach we employ to bound  $\|a\|, \|a^\dagger\|$  is more complex for position and momentum operators.

To obtain error bounds, we leave all expressions in terms of  $\|\hat{x}\|, \|\hat{p}\|$ . We leave a more concrete bound — which can be found by applying a cutoff upon both  $\hat{x}, \hat{p}$  simultaneously — to future work.

### C.1 Conditional rotation gate

**Theorem C.1.** *Suppose we can implement  $e^{it\hat{x}\sigma^i}, e^{it\hat{p}\sigma^i}$  without error. Then, we may approximate  $\mathcal{B}_{\hat{x}^2 + \hat{p}^2}$  with arbitrary error scaling  $p$ :*

$$\left\| \tilde{\mathcal{B}}_{\hat{x}^2 + \hat{p}^2} - \mathcal{B}_{\hat{x}^2 + \hat{p}^2} \right\| \in \mathcal{O}((Ct)^{p+1/2}), \quad (118)$$

where  $C = \max(\|\hat{x}^2 + \hat{p}^2\|, \|\hat{x}\|^2, \|\hat{p}\|^2)$  and using no more than  $4 \cdot 5^{\frac{p}{2} - \frac{1}{4}}$  exponentials.

*Proof.* Begin by directly applying [Theorem B.1](#) to identify the error scaling. This implies that:

$$\left\| \text{BCH}_p(\exp i\tau\hat{x}\sigma^i, \exp i\tau\hat{x}\sigma^j) - \exp \tau^2\hat{x}^2[\sigma^i, \sigma^j] \right\| \in \mathcal{O}((\|\hat{x}\|\tau)^{2p+1}), \quad (119)$$

$$\left\| \text{BCH}_p(\exp i\tau\hat{p}\sigma^i, \exp i\tau\hat{p}\sigma^j) - \exp \tau^2\hat{p}^2[\sigma^i, \sigma^j] \right\| \in \mathcal{O}((\|\hat{p}\|\tau)^{2p+1}). \quad (120)$$

Without loss of generality (WLOG), select  $\sigma^i = \sigma^y$  and  $\sigma^j = \sigma^z$  so that  $[\sigma^i, \sigma^j] = 2i\sigma^x$ . Then, by selecting  $\tau = \sqrt{\frac{t}{2}}$ , the BCH formula is an approximation of  $\mathcal{B}_{\hat{x}^2}(t)$ . Thus,

$$\left\| \tilde{\mathcal{B}}_{\hat{x}^2} - \exp it\hat{x}^2\sigma^x \right\| \in \mathcal{O}((\|\hat{x}\|^2 t)^{p+\frac{1}{2}}). \quad (121)$$

Similarly, for  $\hat{p}^2$ :

$$\left\| \tilde{\mathcal{B}}_{\hat{p}^2} - \exp it\hat{p}^2\sigma^x \right\| \in \mathcal{O}((\|\hat{p}\|^2 t)^{p+\frac{1}{2}}). \quad (122)$$

We apply [Lemma B.2](#) and observe:

$$\left\| \text{Trotter}_q(\tilde{\mathcal{B}}_{\hat{x}^2}, \tilde{\mathcal{B}}_{\hat{p}^2}) - \exp it(\hat{x}^2 + \hat{p}^2)\sigma^x \right\| \in \mathcal{O}((Ct)^{p+\frac{1}{2}}), \quad (123)$$

where  $C = \max(\|\hat{x}^2 + \hat{p}^2\|, \|\hat{x}\|^2, \|\hat{p}\|^2)$  and  $q = \lceil \frac{p}{2} - \frac{1}{4} \rceil$ . This requires no more than  $4 \cdot 5^{q-1}$  operator exponentials, thus implying:

$$4 \cdot 5^{q-1} \leq 4 \cdot 5^{\frac{p}{2} - \frac{1}{4}}. \quad (124)$$

$\square$

## C.2 Controlled-phase beam splitter gate

**Theorem C.2.** Assume we may implement  $e^{it\hat{x}_m\sigma^j}$ ,  $e^{it\hat{p}_m\sigma^j}$  for  $m \in \{1, 2\}$ ; i.e., we may implement the qubit-conditional position shifts and momentum boosts on either mode without error. Then, we may approximate  $\mathcal{B}_{\hat{x}_1\hat{x}_2+\hat{p}_1\hat{p}_2}$  with arbitrary error scaling  $p$ :

$$\left\| \tilde{\mathcal{B}}_{\hat{x}_1\hat{x}_2+\hat{p}_1\hat{p}_2} - \mathcal{B}_{\hat{x}_1\hat{x}_2+\hat{p}_1\hat{p}_2} \right\| \in \mathcal{O}((Ct)^{p+\frac{1}{2}}),$$

where  $C = \max(\|\hat{x}_1\hat{x}_2 + \hat{p}_1\hat{p}_2\|, \|\hat{x}_1\|^2, \|\hat{x}_2\|^2, \|\hat{p}_1\|^2, \|\hat{p}_2\|^2)$  and using no more than  $4 \cdot 5^{\frac{p}{2}-\frac{1}{4}}$  exponentials.

*Proof.* We may take a similar approach as above. Apply [Theorem B.1](#):

$$\left\| \text{BCH}_p(\exp i\tau\hat{x}_1\sigma^i, \exp i\tau\hat{x}_2\sigma^j) - \exp \tau^2\hat{x}_1\hat{x}_2[\sigma^i, \sigma^j] \right\| \in \mathcal{O}((\|\hat{x}\|\tau)^{2p+1}), \quad (125)$$

$$\left\| \text{BCH}_p(\exp i\tau\hat{p}_1\sigma^i, \exp i\tau\hat{p}_2\sigma^j) - \exp \tau^2\hat{p}_1\hat{p}_2[\sigma^i, \sigma^j] \right\| \in \mathcal{O}((\|\hat{p}\|\tau)^{2p+1}), \quad (126)$$

where we set  $\|\hat{x}\| = \max(\|\hat{x}_1\|, \|\hat{x}_2\|)$  and  $\|\hat{p}\| = \max(\|\hat{p}_1\|, \|\hat{p}_2\|)$ . We again take  $\tau = \sqrt{\frac{t}{2}}$  so that:

$$\left\| \tilde{\mathcal{B}}_{\hat{x}_1\hat{x}_2} - \exp it\hat{x}_1\hat{x}_2\sigma^x \right\| \in \mathcal{O}((\|\hat{x}\|^2 t)^{p+\frac{1}{2}}), \quad (127)$$

$$\left\| \tilde{\mathcal{B}}_{\hat{p}_1\hat{p}_2} - \exp it\hat{p}_1\hat{p}_2\sigma^x \right\| \in \mathcal{O}((\|\hat{p}\|^2 t)^{p+\frac{1}{2}}). \quad (128)$$

Applying [Lemma B.2](#):

$$\left\| \text{Trotter}_q(\tilde{\mathcal{B}}_{\hat{x}_1\hat{x}_2}, \tilde{\mathcal{B}}_{\hat{p}_1\hat{p}_2}) - \exp it(\hat{x}_1\hat{x}_2 + \hat{p}_1\hat{p}_2)\sigma^x \right\| \in \mathcal{O}((Ct)^{p+\frac{1}{2}}), \quad (129)$$

where  $C = \max(\|\hat{x}_1\hat{x}_2 + \hat{p}_1\hat{p}_2\|, \|\hat{x}\|^2, \|\hat{p}\|^2)$  and  $q = \lceil \frac{p}{2} - \frac{1}{4} \rceil$ . This requires no more than  $4 \cdot 5^{q-1}$  operator exponentials, thus implying:

$$4 \cdot 5^{q-1} \leq 4 \cdot 5^{\frac{p}{2}-\frac{1}{4}}. \quad (130)$$

□

## D Fock-Space Applications

We now introduce a series of techniques that allow us to realize polynomials of Fock-space operators. We first begin in [Appendix D.1](#) by identifying the error scaling of an arbitrary order Fock-space block encoding, i.e.  $\mathcal{B}_{a^k}$ . In [Appendix D.2](#), we show how the techniques can be used to simulate the Jaynes-Cummings Hamiltonian, which itself is a polynomial of Fock space operators. In [Appendix D.3](#), we demonstrate how this technique can be extended beyond simulation into realizing more general operators, like a state-prep unitary.

### D.1 Realizing block encodings of arbitrary order

We seek to demonstrate the following result:

**Theorem D.1.** For positive integer  $k \geq 1$  and timestep  $t \in \mathbb{R}$ , we seek to implement the target block encoding  $\mathcal{T}_k(t)$  defined as:

$$\mathcal{T}_k(t) = \exp \left( it \begin{bmatrix} 0 & (a^\dagger)^k \\ (a)^k & 0 \end{bmatrix} \right). \quad (131)$$

For any  $\epsilon > 0$  and  $p > 1$  there exists an implementable unitary operation  $\tilde{\mathcal{T}}_{k,p}$  of order  $p$  such that:

$$\left\| \mathcal{T}_k - \tilde{\mathcal{T}}_{k,p} \right\| \leq \epsilon, \quad (132)$$

and the number of applications of  $\mathcal{S}_1(t)$  needed to implement the operation scales in:

$$r \cdot n^{1.6} 30^{np} 420^{n^2 p/2} 6^{\log_2 n + 1}, \quad (133)$$

where  $r \in \Theta \left( \frac{(\Lambda^{k/2} t)^{1+1/(p-1)}}{e^{1/(p-1)}} \right)$ .

Because we can add two lower-order block encodings via [Algorithm 1](#), we can exploit a binary expansion to achieve arbitrary orders (e.g.  $(a^\dagger)^9 = (a^\dagger)^{2^3} a^\dagger$ ). Thus, our first task is to demonstrate the implementation of these block encodings with orders that are a power of two. This is achievable through the recursive POWER algorithm:

---

**Algorithm 3** POWER( $k, t, p$ )

---

**Input:**  $k = 2^\ell$  for nonnegative integer  $\ell$ , timestep  $t > 0$ , order  $p > 1$

**Output:**  $\tilde{\mathcal{T}}_k$  with  $\left\| \tilde{\mathcal{T}}_k - \exp it \begin{bmatrix} 0 & (a^\dagger)^k \\ a^k & 0 \end{bmatrix} \right\| \in \mathcal{O}((\Lambda^{k/2} t)^p)$

if  $k = 1$  then

return  $\mathcal{S}_1(t)$

else

$p' := 2p$

HalfOp := POWER( $k/2, \sqrt{t/2}, p'$ )

return ADD(HalfOp, HalfOp,  $p', p', \sqrt{t/2}$ )

end if

---

Building to the following result:

**Theorem D.2.** For any  $t \geq 0$ ,  $p \geq 1$ , and fixed  $k = 2^\ell$  for some  $\ell \geq 1$  we have that the unitary implemented by [Algorithm 3](#), POWER acting on  $\mathcal{H}_2 \otimes \mathcal{H}_\Lambda$ , satisfies:

$$\left\| \text{POWER}(k, t, p) - \exp \left( it \begin{bmatrix} 0 & (a^\dagger)^k \\ (a)^k & 0 \end{bmatrix} \right) \right\| \in \mathcal{O}((\Lambda^{k/2} t)^p), \quad (134)$$

using no more than  $6^{\log_2 k} \cdot 420^{kp/2}$  unitary  $\mathcal{S}_1$  operators.

To bound the error of this algorithm, we can begin by identifying the implementation error of the second-order formula, i.e.  $\tilde{\mathcal{S}}_2$ , the first operator with implementation error:

**Lemma D.1** (Implementing second-order block encodings). Suppose we can implement the following operation without error (as defined in [Definition 2.1](#) and subject to a bosonic cutoff):

$$\mathcal{S}_1(t) = \exp \left( it \begin{bmatrix} 0 & a^\dagger \\ a & 0 \end{bmatrix} \right). \quad (135)$$

Then, we can approximate  $\mathcal{S}_2(t)$  to the  $p^{\text{th}}$  order, i.e. implement  $\tilde{\mathcal{S}}_2$  such that:

$$\left\| \tilde{\mathcal{S}}_{2,p}(t) - \mathcal{S}_2(t) \right\| \in \mathcal{O}((\Lambda t)^{p+\frac{1}{2}}), \quad (136)$$

using no more than  $6 \cdot 14^p \mathcal{S}_1(t)$  operations.

*Proof.* Note that, if  $\mathcal{S}_1(t)$  is errorless, then we only need to account for error incurred by the BCH and Trotter formulas. By employing a  $p^{\text{th}}$  order BCH formula we can produce commutator exponentials with error  $\mathcal{O}((\Lambda^{1/2}\tau)^{2p+1})$  by [Theorem B.1](#) and [Fact B.3](#).

We again set  $\tau = \sqrt{\frac{t}{2}}$  so that the error scales in at worst  $\mathcal{O}((\Lambda t)^{p+\frac{1}{2}})$ . Then, we apply a Trotter formula [Lemma B.2](#) of order  $\lceil \frac{p}{2} \rceil$  so that:

$$\left\| \exp\left(it \begin{bmatrix} 0 & (a^\dagger)^2 \\ (a)^2 & 0 \end{bmatrix}\right) - \tilde{\mathcal{S}}_2(t) \right\| \in \mathcal{O}((Ct)^{p+\frac{1}{2}}), \quad (137)$$

with  $C \leq \max(\Lambda, \Lambda^{2/2}) = \Lambda$  so that our worst case error scaling is  $\mathcal{O}((\Lambda t)^{p+\frac{1}{2}})$ . This requires no more than  $2 \cdot 2 \cdot 5^{\lceil \frac{p}{2} \rceil - 1}$  of the commutators, each of which required  $8 \cdot 6^{p-1}$  first order operations. Thus, the cost scales in no more than:

$$4 \cdot 5^{p/2} \cdot 8 \cdot 6^{p-1} \leq 6 \cdot 14^p \quad (138)$$

total number of  $\mathcal{S}_1$  operations. □

This base case allows us to analyze the performance of [Algorithm 3](#):

*Proof of [Theorem D.2](#).* We demonstrate the bounds inductively. The base case ( $\ell = 1$ ) holds via [Lemma D.1](#). For the inductive hypothesis, we assume that, for any  $p' \geq 1$  and  $k = 2^\ell$ , we may implement  $\text{POWER}(k, t, p')$ :

$$\left\| \text{POWER}(k, t, p') - \exp\left(it \begin{bmatrix} 0 & (a^\dagger)^k \\ (a)^k & 0 \end{bmatrix}\right) \right\| \in \mathcal{O}((\Lambda^{k/2}t)^{p'}). \quad (139)$$

To demonstrate the inductive step, we seek to apply [Corollary B.2](#) directly to the implementable operators from the inductive hypothesis. Thus, we set  $p' = 2p$  so that:

$$\left\| \text{POWER}(2k, t, p) - \exp\left(it \begin{bmatrix} 0 & (a^\dagger)^{2k} \\ (a)^{2k} & 0 \end{bmatrix}\right) \right\| \in \mathcal{O}((\Lambda^{2k/2}t)^{p'/2}) = \mathcal{O}((\Lambda^{2k/2}t)^p), \quad (140)$$

our desired error scaling. By [Corollary B.2](#), we require an adder of order  $\max(\lceil \frac{p'-1}{2} \rceil, 1) \leq p + \frac{1}{2}$ . Thus, the adder requires  $1.07 \cdot 30^{p+1/2} \leq 6 \cdot 30^p$  of the  $\text{POWER}(k, t, p')$  operations, i.e.:

$$\text{COST}(2k, p) \leq 6 \cdot 30^p \cdot \text{COST}(k, 2p) \quad (141)$$

$$\leq 6 \cdot 30^p \cdot 6 \cdot 30^{2p} \cdot \text{COST}(k/2, 4p) \quad (142)$$

$$\leq \prod_{j=1}^n 6 \cdot 30^{2^{j-1}p} \cdot \text{COST}(2k/2^n, 2^n p) \quad (143)$$

$$\leq 6^\ell \cdot 30^{kp} \cdot \text{COST}(2, kp). \quad (144)$$

Since  $\text{COST}(2, kp) \leq 6 \cdot 14^{kp}$  by [Lemma D.1](#), the number of  $\mathcal{S}_1$  operations is upper bounded by:

$$\text{COST}(2k, p) \leq 6^{\log_2 k + 1} \cdot 420^{kp} \implies \text{COST}(k, p) \leq 6^{\log_2 k} \cdot 420^{kp/2}. \quad (145)$$

□

Together, the POWER and ADD algorithms allow us to approximate arbitrary orders. We describe a recursive algorithm below to construct any order  $k \geq 1$ :

---

**Algorithm 4** ARB\_POWER( $k, t, p, l, r$ ) that produces  $\mathcal{T}_k(t)$  for any  $k \geq 1$

---

**Input:**  $k > 0$  and has the binary representation  $k = k_n k_{n-1} \dots k_1$ .

```

if  $r - l = 0$  then
  if  $k_r = 1$  then
    return POWER( $H, 2^r, t, p$ )
  else
    return  $RX(t) \otimes 1$ 
  end if
else
  return ADD(ARB_POWER( $k, \sqrt{t/2}, p, l, \lfloor \frac{r-l}{2} \rfloor + l$ ), ARB_POWER( $k, \sqrt{t/2}, p, l + \lfloor \frac{r-l}{2} \rfloor + 1, r$ ))
end if

```

---

**Theorem D.3.** Assuming that the  $\mathcal{S}_1$  operator can be implemented without error, the Algorithm 4 produces a series of gates  $\{\mathcal{S}_1(t_i(t))\}$  such that:

$$\left\| \prod_i \mathcal{S}_1(t_i(t)) - \mathcal{T}_k(t) \right\| \in \mathcal{O}((\Lambda^{k/2} t)^p), \quad (146)$$

where  $\mathcal{T}_k$  is our target operator and we have order  $k > 0$ . The number of  $\mathcal{S}_1$  gates required is no more than  $n^{1.6} 30^{np} 420^{n^2 p/2} 6^{\log_2 n + 1}$ .

*Proof.* We demonstrate this constructively on the worst case scenario where  $k = k_n k_{n-1} \dots k_1$  and  $k_n, k_{n-1}, \dots, k_1 = 1$ . WLOG, we assume  $n = 2^\ell$  for some integer  $\ell$ . This is because, if  $n$  not a power of two, we can simply pad the leading digits with zeros to achieve a balanced binary tree.

The proof is as follows: we first identify the error scaling necessary for each leaf node of the binary tree so that the overall formula has our desired order, then we perform the cost accounting and estimate the number of  $\mathcal{S}_1$  operations required.

To achieve an error scaling of  $\mathcal{O}((\Lambda^{2^n/2} t)^p)$ , the two terms being ‘added’ below must have error scaling of order at worst  $\mathcal{O}((\Lambda^{2^n/4} t)^{2p})$  by Corollary B.2, and so on for each subsequent layer. Thus, each of the leaf POWER terms must have order at least  $\mathcal{O}((\Lambda^{2^n/2^{1+\log_2 n}} t)^{2^{\log_2 n} p}) = \mathcal{O}((\Lambda^{2^n/2n} t)^{np})$ .

Now, we compute the cost incurred by the formula. We begin by counting the number of times POWER is used, then accounting for the number of  $\mathcal{S}_1$  required to implement each POWER. Note that each POWER term will be used proportionally to the number of ADD operations necessary, so we can compute the cost of implementing each POWER operation for the  $i^{\text{th}}$  digit, i.e. the POWER operation has degree  $j = 2^i$ . We thus bound the number of  $\mathcal{S}_1$  operations required to implement this  $np^{\text{th}}$ -ordered operator:

$$6^{\log_2 j} \cdot 420^{jnp/2} = 6^i \cdot 420^{2^i np/2}. \quad (147)$$

Finally, we seek to bound the number of times each POWER operator is used through the ADD algorithm. Recall from Corollary B.2 that each ADD operation requires at most  $1.07 \cdot 30^q$  of the constituent operators, where  $q = \max(\lceil \frac{\min(p_l, p_r) - 1}{2} \rceil, 1)$  and  $p_l, p_r$  are the orders of the underlying operators. By assuming symmetry of the Trotter formula for ADD, each addition requires  $\frac{1}{2} 1.07 \cdot 30^q$  of the underlying operator. Thus, we can obtain a bound on the number of applications required

of each fundamental POWER operator:

$$\prod_{s=1}^{\log_2 n} \frac{1}{2} 1.07 \cdot 30^{2^{s-1}p+1/2} \leq 3^{\log_2 n} 30^{np} \leq n^{1.6} 30^{np} \quad (148)$$

because the  $s^{\text{th}}$  layer of ADD requires constituent operators of order  $2^s p$ , so  $q \leq 2^{s-1}p + \frac{1}{2}$ .

Finally, consider the total cost by adding up the cost of the individual POWER operators multiplied by the number of applications required:

$$\sum_{i=1}^{\log_2 n} n^{1.6} 30^{np} \cdot 6^i \cdot 420^{2^i np/2} \leq n^{1.6} 30^{np} 420^{n^2 p/2} \sum_{i=1}^{\log_2 n} 6^i \quad (149)$$

$$\leq n^{1.6} 30^{np} 420^{n^2 p/2} 6^{\log_2 n + 1}, \quad (150)$$

as desired.  $\square$

Now, we seek to finalize the number of ops required in terms of  $\epsilon$ . Recognize that we may use timeslicing to reduce the error arbitrarily. Note that:

**Lemma D.2.** *Suppose we may implement  $\tilde{\mathcal{T}}_{k,p}(t)$ , an approximation of  $\mathcal{T}_k(t)$  with  $p > 1$  such that:*

$$\left\| \mathcal{T}_k(t) - \tilde{\mathcal{T}}_{k,p}(t) \right\| \in \mathcal{O}((\Lambda^{k/2}t)^p). \quad (151)$$

*Then, by timeslicing the approximation, we can produce  $\tilde{\mathcal{T}}_{k,p}^r(t)$  where:*

$$\left\| \mathcal{T}_k(t) - \tilde{\mathcal{T}}_{k,p}^r(t) \right\| \leq \epsilon, \quad (152)$$

*where  $\tilde{\mathcal{T}}_k^r(t)$  requires  $r \in \Theta\left(\frac{(\Lambda^{k/2}t)^{1+1/(p-1)}}{\epsilon^{1/(p-1)}}\right)$  applications of the  $\tilde{\mathcal{T}}_k(t)$  operator.*

*Proof.* We define the timeslicing of  $\tilde{\mathcal{T}}_k(t)$  as applying  $\tilde{\mathcal{T}}_k(t/r)$  operator  $r$  times:

$$\tilde{\mathcal{T}}_{k,p}^r(t) = \tilde{\mathcal{T}}_{k,p}(t/r)^r. \quad (153)$$

To find a Taylor expansion for  $\tilde{\mathcal{T}}_{k,p}(t/r)^r$ , note the explicit form for  $\tilde{\mathcal{T}}_{k,p}(t)$ :

$$\tilde{\mathcal{T}}_{k,p}(t) = e^{iA_k t} + \Delta(t)(\Lambda^{k/2}t)^p, \quad (154)$$

where  $\|\Delta(t)\| \in \mathcal{O}(1)$ . This allows us to express the refined operator as follows:

$$\tilde{\mathcal{T}}_k(t/r)^r = \left( e^{iA_k t/r} + \Delta\left(\frac{t}{r}\right) \left(\frac{t^p}{r^p}\right) \right)^r \quad (155)$$

$$= e^{iA_k t} + \left[ \sum_{j=1}^{r-1} (e^{iA_k t/r})^j \Delta\left(\frac{t}{r}\right) (e^{iA_k t/r})^{r-1-j} \right] \left( \frac{(\Lambda^{k/2}t)^p}{r^p} \right) + \mathcal{O}\left( \left( \frac{(\Lambda^{k/2}t)^p}{r^p} \right)^{p+1} \right), \quad (156)$$

Thus, when we analyze the error:

$$\begin{aligned} \left\| \mathcal{T}_k(t/r)^r - e^{iA_k t} \right\| &\leq \mathcal{O}\left( r \left\| (e^{iA_k t/r})^{r-1} \right\| \left\| \Delta\left(\frac{t}{r}\right) \right\| \left( \frac{(\Lambda^{k/2}t)^p}{r^p} \right) \right) \\ &\subset \mathcal{O}\left( \frac{(\Lambda^{k/2}t)^p}{r^{p-1}} \right). \end{aligned} \quad (157)$$



To bound the implementation error by  $\epsilon$ , i.e.  $\epsilon \in \mathcal{O}\left(\frac{(\Lambda^{k/2}t)^p}{r^{p-1}}\right)$ , we should select  $r$  as follows:

$$r \in \Theta\left(\frac{(\Lambda^{k/2}t)^{p/(p-1)}}{\epsilon^{1/(p-1)}}\right) = \Theta\left(\frac{(\Lambda^{k/2}t)^{1+1/(p-1)}}{\epsilon^{1/(p-1)}}\right), \quad (158)$$

as desired.  $\square$

Finally, we can demonstrate our original theorem statement, allowing us to create a bound on the number of  $\mathcal{S}_1$  operations necessary to achieve an arbitrarily ordered operator:

*Proof of Theorem D.1.* By Theorem D.3, we can perform a single Trotter step of timestep  $\frac{t}{r}$  using  $n^{1.6}30^{np}420^{n^2p/2}6^{\log_2 n+1}$   $\mathcal{S}_1$  operations. Thus, the total number of  $\mathcal{S}_1$  operations required scales in:

$$r \cdot n^{1.6}30^{np}420^{n^2p/2}6^{\log_2 n+1}, \quad (159)$$

where, by Lemma D.2, it is sufficient to set  $r \in \Theta\left(\frac{(\Lambda^{k/2}t)^{1+1/(p-1)}}{\epsilon^{1/(p-1)}}\right)$ .  $\square$

## D.2 Generation of nonlinear Hamiltonians

**Theorem D.4.** *Let  $H = \omega a^\dagger a + \frac{\kappa}{2}(a^\dagger)^2 a^2$ ,  $t$  be an evolution time and  $\epsilon$  be an error tolerance. For any positive integer  $q$  we can approximate an exponential of the block-encoded Hamiltonian with error at most  $\epsilon$  in the operator norm using  $re^{\mathcal{O}(q)}$   $\mathcal{S}_1$  operations where  $r \in \Omega\left(\frac{(\Lambda^4 t)^{1+1/(q-\frac{3}{4})}}{\epsilon^{1/(q-\frac{3}{4})}}\right)$ .*

*Proof.* We first show that the two Hamiltonian terms are implementable separately. Then, via Trotter, we combine them and perform an error analysis. In particular, we hope to embed the Hamiltonian such that we approximate the following operator:

$$\exp it \begin{bmatrix} H & 0 \\ 0 & \cdot \end{bmatrix}, \quad (160)$$

i.e., where the Hamiltonian is embedded in the upper left hand block. Thus, when applied to a system with the  $|0\rangle$  qubit, this amounts to implementing  $\exp itH$  on the mode.

We begin by embedding the  $a^\dagger a$  term. Notice that  $a^\dagger a$  Hermitian; thus, we can apply Algorithm 2 on the  $a, a^\dagger$  block encodings. By the error analysis in Theorem B.1 and the bound on norm from Fact B.3:

$$\left\| \text{BCH}_q(\mathcal{S}_1^Y(\tau), \mathcal{S}_1(\tau)) - \exp 2i\tau^2 \begin{bmatrix} a^\dagger a & 0 \\ 0 & aa^\dagger \end{bmatrix} \right\| \in \mathcal{O}((\Lambda^{1/2}\tau)^{2q+1}), \quad (161)$$

so that, by setting  $\tau = \sqrt{\frac{\omega t}{2}}$ , we have:

$$\left\| \text{BCH}_q\left(\mathcal{S}_1^Y\left(\sqrt{\frac{\omega t}{2}}\right), \mathcal{S}_1\left(\sqrt{\frac{\omega t}{2}}\right)\right) - \exp i\omega t \begin{bmatrix} a^\dagger a & 0 \\ 0 & aa^\dagger \end{bmatrix} \right\| \in \mathcal{O}((\Lambda\omega t)^{q+\frac{1}{2}}), \quad (162)$$

using  $8 \cdot 6^{q-1}$  total  $\mathcal{S}_1$  operations.

Recall that we can easily block-encode  $(a^\dagger)^2$  and  $(a)^2$  via [Algorithm 3](#). We then apply [Algorithm 2](#) to  $(a^\dagger)^2, a^2$  to yield the desired upper-left block encoding. Namely, because we can implement  $\mathcal{S}_{2,p}$  with the following error scaling:

$$\left\| \mathcal{S}_{2,p}(\tau) - \exp i\tau \begin{bmatrix} 0 & (a^\dagger)^2 \\ a^2 & 0 \end{bmatrix} \right\| \in \mathcal{O}((\Lambda\tau)^{p+\frac{1}{2}}), \quad (163)$$

using no more than  $6 \cdot 14^p$   $\mathcal{S}_1$  operations, we can apply [Algorithm 2](#) to find:

$$\left\| \text{MULT}(\mathcal{S}_{2,p}(\tau), X\mathcal{S}_{2,p}(\tau)X) - \exp 2i\tau^2 \begin{bmatrix} (a^\dagger)^2(a)^2 & 0 \\ 0 & (a)^2(a^\dagger)^2 \end{bmatrix} \right\| \in \mathcal{O}((\Lambda^2\tau)^{p+\frac{1}{2}}), \quad (164)$$

by setting  $\ell = \lceil \frac{p-\frac{1}{2}}{2} \rceil \leq \frac{p}{2} + 1$  and thus using  $8 \cdot 6^{\ell-1}$  exponentials. When  $\tau = \sqrt{\frac{\kappa t}{4}}$ :

$$\left\| \text{BCH}_\ell \left( \mathcal{S}_{2,p}^Y \left( \sqrt{\frac{\kappa t}{4}} \right), \mathcal{S}_{2,p} \left( \sqrt{\frac{\kappa t}{4}} \right) \right) - \exp i\frac{\kappa}{2}t \begin{bmatrix} (a^\dagger)^2(a)^2 & 0 \\ 0 & (a)^2(a^\dagger)^2 \end{bmatrix} \right\| \in \mathcal{O}((\Lambda^4\kappa t)^{\frac{p}{2}+\frac{1}{4}}), \quad (165)$$

using no more than  $8 \cdot 6^{\ell-1} \cdot 6 \cdot 14^p \leq 48 \cdot 6^{p/2} \cdot 14^p \leq 48 \cdot 35^p$  total  $\mathcal{S}_1$  operators. Then, we may set  $p = 2q$  so that, given no more than  $48 \cdot 35^{2q}$  total  $\mathcal{S}_1$  operations, we can implement the BCH formula with error scaling  $\mathcal{O}((\Lambda^4\kappa t)^{q+\frac{1}{4}})$ .

Finally, we apply the Trotter formula to the two subterms via [Lemma B.2](#), finding:

$$\left\| \text{Trotter}_{2s} \left( \text{BCH}_q \left( \mathcal{S}_X^Y \left( \sqrt{\frac{\omega t}{2}} \right), \mathcal{S}_X \left( \sqrt{\frac{\omega t}{2}} \right) \right), \text{BCH}_u \left( \mathcal{S}_{2,p}^Y \left( \sqrt{\frac{\kappa t}{4}} \right), \mathcal{S}_{2,p} \left( \sqrt{\frac{\kappa t}{4}} \right) \right) \right) - \exp it \begin{bmatrix} H & 0 \\ 0 & \cdot \end{bmatrix} \right\| \quad (166)$$

$$\in \mathcal{O}((\Lambda^4 \max(\omega, \kappa)t)^{q+\frac{1}{4}}), \quad (167)$$

where the constant factor can be obtained by observing the Hamiltonian norm is bounded via the triangle inequality. Now, by setting  $s = \lceil \frac{1}{2}(q - \frac{3}{4}) \rceil \leq \frac{q}{2} + \frac{5}{8}$ , we can obtain the desired error scaling. This formula requires no more than  $4 \cdot 5^{s-1}$  total operations; by symmetry, we can assume each of the BCH formulas only must be applied  $2 \cdot 5^{s-1}$  times. Thus, the total number of  $\mathcal{S}_1$  operations is no more than:

$$2 \cdot 5^{s-1} (8 \cdot 6^{q-1} + 48 \cdot 35^{2q}) \leq 4 \cdot 5^{\frac{q}{2}} \cdot 48 \cdot 35^{2q} \leq 192 \cdot 2900^q. \quad (168)$$

To produce an  $\epsilon$  scaling, we apply [Lemma D.2](#) to the Trotterized operator, implying that we require the following  $r$  scaling for fixed  $q$ :

$$r \in \Omega \left( \frac{(\Lambda^4 t)^{1+1/(q-\frac{3}{4})}}{\epsilon^{1/(q-\frac{3}{4})}} \right), \quad (169)$$

where the total number of  $\mathcal{S}_1$  operations is no more than:

$$r \cdot 192 \cdot 2900^q \subset r e^{\mathcal{O}(q)}. \quad (170)$$

□

### D.3 Application to state preparation

We first need to demonstrate the connection between block-encoded powers of annihilation/creation operators and state preparation. First, observe that the ideal block encoding would allow for initialization from the vacuum:

**Theorem D.5.** *For  $k \leq \Lambda$ , we can take  $t = (2n + 1)\frac{\pi}{2\sqrt{k!}}$  for any  $n \in \mathbb{N}$  so that:*

$$\mathcal{T}_k(t) |1\rangle \otimes |0\rangle = |0\rangle \otimes |k\rangle.$$

*Proof.* The proof is algebraic; begin by producing the Taylor series expansion of the operator:

$$\mathcal{T}_k(t) = \exp\left(it \begin{bmatrix} 0 & (a^\dagger)^k \\ (a)^k & 0 \end{bmatrix}\right) \quad (171)$$

$$= \sum_{j=0}^{\infty} \frac{(it)^j}{j!} \begin{bmatrix} 0 & (a^\dagger)^k \\ (a)^k & 0 \end{bmatrix}^j \quad (172)$$

$$= \sum_{j=0}^{\infty} \frac{(it)^{2j}}{(2j)!} \begin{bmatrix} 0 & (a^\dagger)^k \\ (a)^k & 0 \end{bmatrix}^{2j} + \sum_{j=0}^{\infty} \frac{(it)^{2j+1}}{(2j+1)!} \begin{bmatrix} 0 & (a^\dagger)^k \\ (a)^k & 0 \end{bmatrix}^{2j+1}, \quad (173)$$

where the matrix products have well-defined forms:

$$\begin{bmatrix} 0 & (a^\dagger)^k \\ (a)^k & 0 \end{bmatrix}^{2j} = \begin{bmatrix} ((a^\dagger)^k (a)^k)^j & 0 \\ 0 & ((a)^k (a^\dagger)^k)^j \end{bmatrix}, \quad (174)$$

$$\begin{bmatrix} 0 & (a^\dagger)^k \\ (a)^k & 0 \end{bmatrix}^{2j+1} = \begin{bmatrix} 0 & (a^\dagger)^k ((a)^k (a^\dagger)^k)^j \\ (a)^k ((a^\dagger)^k (a)^k)^j & 0 \end{bmatrix}, \quad (175)$$

so that:

$$\exp\left(it \begin{bmatrix} 0 & (a^\dagger)^k \\ (a)^k & 0 \end{bmatrix}\right) |1\rangle \otimes |0\rangle \quad (176)$$

$$= \sum_{j=0}^{\infty} \frac{(it)^{2j}}{(2j)!} \sqrt{k!}^{2j} |1\rangle \otimes |0\rangle + \sum_{j=0}^{\infty} \frac{(it)^{2j+1}}{(2j+1)!} \sqrt{k!}^{2j+1} |0\rangle \otimes |k\rangle \quad (177)$$

$$= \cos(t\sqrt{k!}) |1\rangle \otimes |0\rangle + i \sin(t\sqrt{k!}) |0\rangle \otimes |k\rangle. \quad (178)$$

When  $t\sqrt{k!} = (2n + 1)\frac{\pi}{2}$  for  $n \in \mathbb{N}$ , the  $|1\rangle \otimes |0\rangle$  term vanishes and we are left with the  $|0\rangle \otimes |k\rangle$  Fock state, as desired.  $\square$

While this result allows us to prepare the  $|k\rangle$  Fock state, it also will incur unwanted transformations on starting states other than the vacuum ( $|1\rangle \otimes |n\rangle, n \neq 1$ ). By applying the BCH formula, we can isolate this operation so that it only operates on the  $|1\rangle \otimes |0\rangle$  term. In particular, we argue:

**Theorem D.6.** *Consider the Fock preparation unitary  $\mathcal{P}_k$  with the following form:*

$$\exp\left(it \begin{bmatrix} 0 & (a^\dagger)^k |0\rangle\langle 0| \\ |0\rangle\langle 0| (a)^k & 0 \end{bmatrix}\right).$$

When  $t = (2n + 1) \frac{\pi}{4\sqrt{k!}}$ , we have that  $\mathcal{P}_k$  performs our desired state preparation:

$$\exp \left( it \begin{bmatrix} 0 & (a^\dagger)^k |0\rangle\langle 0| \\ |0\rangle\langle 0| (a)^k & 0 \end{bmatrix} \right) |1\rangle \otimes |b\rangle = \begin{cases} |0\rangle \otimes |k\rangle & b = 0 \\ |1\rangle \otimes |b\rangle & b \neq 0 \end{cases}.$$

We claim that we can approximate this unitary with  $\tilde{\mathcal{P}}_{k,p}$  where:

$$\left\| \tilde{\mathcal{P}}_{k,p} - \mathcal{P}_k \right\| \in \mathcal{O}((\Lambda^{k/2}t)^p),$$

using no more than  $4 \cdot 5^{q-1} \tilde{\mathcal{T}}_{k,p}$  subroutines.

*Proof.* The general construction of the operator emerges from the use of a Trotter formula in conjunction with a phase rotation gate. Begin by defining the rotation operator:

**Definition D.7.** Call  $R_{Z0}$  the phase-flip operator acting on some set of modes  $B$  to be:

$$R_{Z0} := \mathbf{1} \otimes (\mathbf{1} - 2|0\rangle\langle 0|), \quad (179)$$

i.e., only flip the phase for the vacuum. This operator is implementable using a 0-controlled cavity-conditioned qubit rotation gate.

Then, because  $R_{Z0}$  is self-adjoint, we can conjugate  $\mathcal{T}_k(-t)$  without error as follows:

$$R_{Z0} \mathcal{T}_k(-t) R_{Z0} = R_{Z0} \exp \left( it' \begin{bmatrix} 0 & (a^\dagger)^k \\ (a)^k & 0 \end{bmatrix} \right) R_{Z0} \quad (180)$$

$$= \exp \left( -it R_{Z0} \begin{bmatrix} 0 & (a^\dagger)^k \\ (a)^k & 0 \end{bmatrix} R_{Z0} \right) \quad (181)$$

$$= \exp \left( it \begin{bmatrix} 0 & (a^\dagger)^k (2|0\rangle\langle 0| - \mathbf{1}) \\ (2|0\rangle\langle 0| - \mathbf{1})(a)^k & 0 \end{bmatrix} \right), \quad (182)$$

where specific left- and right-hand  $(2|0\rangle\langle 0| - \mathbf{1})$  terms vanish given the annihilation/creation operators. We then apply the Trotter formula upon  $\mathcal{T}_k(t/2), R_{Z0} \mathcal{T}_k(-t/2) R_{Z0}$ , yielding:

$$\exp \left( it \begin{bmatrix} 0 & (a^\dagger)^k |0\rangle\langle 0| \\ |0\rangle\langle 0| (a)^k & 0 \end{bmatrix} \right), \quad (183)$$

as desired.

To compute the error scaling, recall our result from [Theorem D.3](#) which states the error scaling of  $\tilde{\mathcal{T}}_{k,p}$  (and, respectively,  $R_{Z0} \tilde{\mathcal{T}}_{k,p} R_{Z0}$ ):

$$\left\| \tilde{\mathcal{T}}_{k,p}(t) - \mathcal{T}_k(t) \right\| \in \mathcal{O}((\Lambda^{k/2}t)^p), \quad (184)$$

so that, by [Lemma B.2](#),

$$\left\| \text{Trotter}_{2q}(\tilde{\mathcal{T}}_{k,p}(t/2), R_{Z0} \tilde{\mathcal{T}}_{k,p}(-t/2) R_{Z0}) - \exp \left( it \begin{bmatrix} 0 & (a^\dagger)^k |0\rangle\langle 0| \\ |0\rangle\langle 0| (a)^k & 0 \end{bmatrix} \right) \right\| \in \mathcal{O}((\Lambda^{k/2}t)^p), \quad (185)$$

when  $q = \max(\lceil \frac{p-1}{2} \rceil, 1)$  and using no more than  $4 \cdot 5^{q-1}$  operator exponentials. Thus, we can set  $q = \frac{p+1}{2} \geq \max(\lceil \frac{p-1}{2} \rceil, 1)$  so that we use no more than  $4 \cdot 5^{\frac{p-1}{2}} \leq 2 \cdot 5^{p/2} \tilde{\mathcal{T}}_{k,p}$  terms.  $\square$

Thus, our approximate operators can be applied to yield the same result with high probability:

**Theorem D.8.** *We can prepare the  $|0\rangle \otimes |k\rangle$  with probability at least  $1 - \delta$  using no more than  $r \in \Theta\left(\frac{(\Lambda^{k/2}t)^{1+1/(p-1)}}{(\delta/2)^{1/(p-1)}}\right)$   $\mathcal{F}_{k,p}$  operators or at most*

$$r \cdot 2 \cdot 5^{p/2} \cdot n^{1.6} 30^{np} 420^{n^2 p/2} 6^{\log_2 n+1} \quad (186)$$

$\mathcal{S}_1$  operators.

*Proof.* Begin by identifying the  $\epsilon$  precision necessary to yield a failure probability less than  $\delta$ . A sufficient condition would be that:

$$\left| \left\| |0\rangle\langle 0| \otimes |k\rangle\langle k| \tilde{\mathcal{P}}_{k,p} |1\rangle \otimes |0\rangle \right\|^2 - \left\| |0\rangle\langle 0| \otimes |k\rangle\langle k| \mathcal{P}_k |1\rangle \otimes |0\rangle \right\|^2 \right| \leq \delta. \quad (187)$$

Observe that our idealized operator has a success probability; thus, we seek to demonstrate that:

$$\left| \left\| |0\rangle\langle 0| \otimes |k\rangle\langle k| \tilde{\mathcal{P}}_{k,p} |1\rangle \otimes |0\rangle \right\|^2 - 1 \right| \leq \delta. \quad (188)$$

Because the probability of measuring  $|0\rangle \otimes |k\rangle$  lies in  $[0, 1]$ , the above inequality holds when:

$$\left\| |0\rangle\langle 0| \otimes |k\rangle\langle k| \tilde{\mathcal{P}}_{k,p} |1\rangle \otimes |0\rangle \right\|^2 \geq 1 - \delta. \quad (189)$$

Recognize that we can lower bound the norm:

$$\left\| |0\rangle\langle 0| \otimes |k\rangle\langle k| \tilde{\mathcal{P}}_{k,p} |1\rangle \otimes |0\rangle \right\| \quad (190)$$

$$= \left\| |0\rangle\langle 0| \otimes |k\rangle\langle k| (\mathcal{P}_k - (\mathcal{P}_k - \tilde{\mathcal{P}}_{k,p})) |1\rangle \otimes |0\rangle \right\| \quad (191)$$

$$\geq \left\| |0\rangle\langle 0| \otimes |k\rangle\langle k| \mathcal{F}_k |1\rangle \otimes |0\rangle \right\| - \left\| |0\rangle\langle 0| \otimes |k\rangle\langle k| (\mathcal{P}_k - \tilde{\mathcal{P}}_{k,p}) |1\rangle \otimes |0\rangle \right\| \quad (192)$$

$$\geq 1 - \left\| \mathcal{P}_k - \tilde{\mathcal{P}}_{k,p} \right\|_\infty. \quad (193)$$

By requiring  $\left\| \mathcal{P}_k - \tilde{\mathcal{P}}_{k,p} \right\|_\infty \leq 1$ . This allows us to produce a lower bound on the original LHS:

$$\left\| |0\rangle\langle 0| \otimes |k\rangle\langle k| \tilde{\mathcal{P}}_{k,p} |1\rangle \otimes |0\rangle \right\|^2 \geq 1 - 2 \left\| \mathcal{P}_k - \tilde{\mathcal{P}}_{k,p} \right\|_\infty. \quad (194)$$

Thus, it is sufficient for the following to hold:

$$1 - 2 \left\| \mathcal{P}_k - \tilde{\mathcal{P}}_{k,p} \right\|_\infty \geq 1 - \delta \iff \left\| \mathcal{P}_k - \tilde{\mathcal{P}}_{k,p} \right\|_\infty \leq \frac{\delta}{2}. \quad (195)$$

Apply [Lemma D.2](#) to [Theorem D.6](#) so that the time-sliced  $\tilde{\mathcal{P}}_{k,p}^r$  has:

$$\left\| \tilde{\mathcal{P}}_{k,p}^r - \mathcal{P}_k \right\| \leq \frac{\delta}{2}, \quad (196)$$

by using  $r \in \Theta\left(\frac{(\Lambda^{k/2}t)^{1+1/(p-1)}}{(\delta/2)^{1/(p-1)}}\right)$  applications of  $\tilde{\mathcal{P}}_{k,p}(t/r)$ . The  $\mathcal{S}_1$  bound follows from a similar analysis to [Theorem D.1](#) applied to the result from [Theorem D.6](#). □

## E Universal Control of the Span $\{|0\rangle, |1\rangle\}$ Fock Space

To demonstrate the efficacy of the instruction set, we demonstrate the use of the approach to encode a qubit in a cavity either via generation of effective Pauli gates or imposition of an effective Hubbard interaction in the Jaynes-Cumming Hamiltonian. In this sense, the techniques presented here are analogous to those in [34], in that we use our results to effectively truncate the quantum information to a two-dimensional subspace despite the fact that the natural dynamics of the systems causes the quantum information to leak from this space into the larger Hilbert space of the cavity.

For universal control in the restricted span  $\{|0\rangle, |1\rangle\}$  Hilbert space, we generate three effective Pauli operators  $\sigma_{\text{eff}}^x$ ,  $\sigma_{\text{eff}}^y$ , and  $\sigma_{\text{eff}}^z$  that produce Pauli rotations in the lowest two modes of the cavity, with minimal leakage to higher energy states. The form of the effective Pauli operators is determined by expressing the standard Pauli operators

$$\sigma^x = \begin{pmatrix} 0 & 1 \\ 1 & 0 \end{pmatrix}, \quad (197)$$

$$\sigma^y = \begin{pmatrix} 0 & -i \\ i & 0 \end{pmatrix}, \quad (198)$$

$$\sigma^z = \begin{pmatrix} 1 & 0 \\ 0 & -1 \end{pmatrix}, \quad (199)$$

in terms of creation and annihilation operators truncated to the first two Fock states

$$\hat{a}_{\text{eff}}^\dagger = \begin{pmatrix} 0 & 0 \\ 1 & 0 \end{pmatrix}, \quad (200)$$

$$\hat{a}_{\text{eff}} = \begin{pmatrix} 0 & 1 \\ 0 & 0 \end{pmatrix}, \quad (201)$$

$$\hat{n}_{\text{eff}} = \hat{a}_{\text{eff}}^\dagger \hat{a}_{\text{eff}} = \begin{pmatrix} 0 & 0 \\ 0 & 1 \end{pmatrix}, \quad (202)$$

which yields

$$\sigma_{\text{eff}}^x = \hat{a}_{\text{eff}}^\dagger + \hat{a}_{\text{eff}}, \quad (203)$$

$$\sigma_{\text{eff}}^y = i \left( \hat{a}_{\text{eff}}^\dagger - \hat{a}_{\text{eff}} \right), \quad (204)$$

$$\sigma_{\text{eff}}^z = I - 2\hat{a}_{\text{eff}}^\dagger \hat{a}_{\text{eff}}. \quad (205)$$

To reduce leakage into higher energy states, we ensure the creation operator  $\hat{a}_{\text{eff}}^\dagger$  only acts on the ground state  $|0\rangle$  and the annihilation operator  $\hat{a}_{\text{eff}}$  only acts on the first excited state  $|1\rangle$  with the projector

$$\hat{P}_0 \approx I - \hat{n} \quad (206)$$

$$= \begin{cases} 0 & n = 1 \\ 1 & n = 0 \end{cases}, \quad (207)$$

where  $n$  is the number of photons in the cavity and where only the span  $\{|0\rangle, |1\rangle\}$  states are populated. Since the operator is a projector, it obeys the relation

$$\hat{P}_0^2 = \hat{P}_0, \quad (208)$$

such that the effective Pauli gates are

$$\sigma_{\text{eff}}^x = \hat{a}_{\text{eff}}^\dagger \hat{P}_0 + \hat{P}_0 \hat{a}_{\text{eff}} \quad (209)$$

$$\approx \hat{a}^\dagger (I - \hat{n}) + (I - \hat{n}) \hat{a}, \quad (210)$$

$$\sigma_{\text{eff}}^y = i \left( \hat{a}_{\text{eff}}^\dagger \hat{P}_0 - \hat{P}_0 \hat{a}_{\text{eff}} \right) \quad (211)$$

$$\approx i \left( \hat{a}^\dagger (I - \hat{n}) - (I - \hat{n}) \hat{a} \right), \quad (212)$$

$$\sigma_{\text{eff}}^z = I - 2\hat{a}_{\text{eff}}^\dagger \hat{P}_0^2 \hat{a}_{\text{eff}} \quad (213)$$

$$\approx I - 2\hat{a}^\dagger (I - \hat{n}) \hat{a}. \quad (214)$$

## Pauli X Gate

Consider the infinitesimal  $\sigma_x$ -rotation gate in the span  $\{|0\rangle, |1\rangle\}$  Fock space

$$U_{\text{span}\{0,1\},x} = e^{i\lambda^2 \sigma_{\text{eff}}^x \sigma^z} \quad (215)$$

$$= e^{i\lambda^2 (\hat{a}^\dagger (1-\hat{n}) + (1-\hat{n}) \hat{a}) \sigma^z}. \quad (216)$$

Expression of the exponent in terms of phase-space operators Eq. 55, Eq. 4, and Eq. 3 gives

$$\begin{aligned} & i\lambda^2 \left( \hat{a}^\dagger (I - \hat{n}) + (I - \hat{n}) \hat{a} \right) \sigma^z \\ &= i\lambda^2 (2\hat{x} - \{\hat{x}, \hat{n}\} + i[\hat{p}, \hat{n}]) \sigma^z. \end{aligned} \quad (217)$$

The gate is therefore given by a Trotter-Suzuki decomposition of three terms:  $\exp\left(\left[\hat{A}_1, \hat{B}_1\right] \lambda^2\right) = \exp(-i\lambda^2 \{\hat{x}, \hat{n}\} \sigma^z)$ ,  $\exp\left(\left[\hat{A}_2, \hat{B}_2\right] \lambda^2\right) = \exp(-\lambda^2 [\hat{p}, \hat{n}] \sigma^z)$ , and  $\exp(2i\lambda^2 \hat{x} \sigma^z)$ .

The terms consisting of exponentials of commutators are decomposed via BCH. The relationship between the commutator and anticommutator required for the first term is given by the Pauli anticommutation-commutation relation

$$-i \{\hat{x}, \hat{n}\} \sigma^z = -i (i [\hat{x} \sigma^x, \hat{n} \sigma^y]) \quad (218)$$

$$= [i\hat{x} \sigma^x, i\hat{n} \sigma^y] \quad (219)$$

$$= [\hat{A}_1, \hat{B}_1], \quad (220)$$

where  $\hat{A}_1$  corresponds to a position displacement and  $\hat{B}_1$  corresponds to the  $y$ -conditional rotation gate. The argument of the second term is already in the form of a commutator, such that

$$[\hat{A}_2, \hat{B}_2] = -[\hat{p}, \hat{n}] \sigma^z \quad (221)$$

$$= [i\hat{p}, i\hat{n} \sigma^z], \quad (222)$$

where  $\hat{A}_2$  corresponds to an *unconditional* momentum boost, and  $\hat{B}_2$  corresponds to the  $z$ -conditional rotation gate. Lastly, the third term already belongs to the instruction set architecture and needs no further decomposition.

The infinitesimal  $\sigma_x$ -rotation gate in the span  $\{|0\rangle, |1\rangle\}$  Fock space is therefore composed of a product of nine rotation and displacement gates or 21 displacement gates.

## Pauli Y Gate

The infinitesimal  $\sigma_y$ -rotation gate in the span  $\{|0\rangle, |1\rangle\}$  Fock space is determined analogously

$$U_{\text{span}\{0,1\},y} = e^{i\lambda^2 \sigma_{\text{eff}}^y \sigma^z} \quad (223)$$

$$= e^{-\lambda^2 (\hat{a}^\dagger (I - \hat{n}) + (I - \hat{n}) \hat{a}) \sigma^z}. \quad (224)$$

Expression of the argument of the exponent in terms of phase-space variables Eq. 4 and Eq. 3 yields

$$\begin{aligned} & -\lambda^2 \left( \hat{a}^\dagger (I - \hat{n}) - (I - \hat{n}) \hat{a} \right) \sigma^z \\ & = -\lambda^2 (-2i\hat{p} + [\hat{n}, \hat{x}] + i\{\hat{n}, \hat{p}\}) \sigma^z, \end{aligned} \quad (225)$$

such that the gate is a Trotter-Suzuki decomposition of  $\exp\left(\left[\hat{A}_1, \hat{B}_1\right] \lambda^2\right) = \exp(-\lambda^2 [n, x] \sigma^z)$ ,  $\exp\left(\left[\hat{A}_2, \hat{B}_2 \lambda^2\right]\right) = \exp(-i\lambda^2 \{p, n\} \sigma^z)$ , and  $\exp(2i\lambda^2 p \sigma^z)$ .

Again, the first two exponential terms are decomposed via the BCH formula . The first commutator is

$$\left[\hat{A}_1, \hat{B}_1\right] = [\hat{n}, \hat{x}] \sigma^z \quad (226)$$

$$= [\hat{n} \sigma^z, \hat{x}], \quad (227)$$

where the exponent of  $\hat{A}_1$  is a  $z$ -conditional rotation gate and the exponent of  $\hat{B}_1$  is an unconditional position displacement. The second commutator is given by the Pauli anticommutation-relation:

$$i\{p, n\} \sigma^z = i(i[ip\sigma^x, in\sigma^y]) \quad (228)$$

$$= [ip\sigma^x, in\sigma^y] \quad (229)$$

$$= \left[\hat{A}_2, \hat{B}_2\right], \quad (230)$$

where the exponent of  $\hat{A}_2$  corresponds to a conditional momentum shift and the exponent of  $\hat{B}_2$  is a  $y$ -conditional rotation gate.

The infinitesimal  $\sigma_y$ -rotation gate in the span  $\{|0\rangle, |1\rangle\}$  Fock space therefore has a lower bound gate depth of nine displacement and rotation gates or 21 in displacement gates.

## Pauli Z Gate

The infinitesimal  $\sigma_z$ -rotation gate in the span  $\{|0\rangle, |1\rangle\}$  Fock space is

$$U_{\text{span}\{0,1\},z} = e^{i\lambda^2 \sigma_{\text{eff}}^z \sigma^z} \quad (231)$$

$$= e^{-\lambda^2 (I - 2\hat{a}^\dagger (I - \hat{n}) \hat{a}) \sigma^z}, \quad (232)$$

whose argument in terms of ladder operators is

$$\begin{aligned} & -\lambda^2 \left( I - 2\hat{a}^\dagger (I - \hat{n}) \hat{a} \right) \sigma^z \\ & = -\lambda^2 \left( I - 2\hat{a}^\dagger \hat{a} + 2\hat{a}^\dagger \hat{a}^\dagger \hat{a} \hat{a} \right) \sigma^z, \end{aligned} \quad (233)$$



Given the ladder operator commutator Eq. 6,

$$\hat{a}^\dagger \hat{a} = \hat{a} \hat{a}^\dagger - I, \quad (234)$$

the relationship between the fourth-order ladder operator term and the number operator is

$$\hat{a}^\dagger \hat{a}^\dagger \hat{a} \hat{a} = \hat{a}^\dagger (\hat{a} \hat{a}^\dagger - I) \hat{a} \quad (235)$$

$$= \hat{a}^\dagger \hat{a} \hat{a}^\dagger \hat{a} - \hat{a}^\dagger \hat{a} \quad (236)$$

$$= \hat{n}^2 - \hat{n}. \quad (237)$$

The argument of the exponential in terms of number operators is then

$$-\lambda^2 (I - 2\hat{a}^\dagger (I - \hat{n}) \hat{a}) \sigma^z = -\lambda^2 (I - 4\hat{n} + 2\hat{n}^2) \sigma^z. \quad (238)$$

The argument is further simplified given that the state is restricted to the first two cavity modes, as for  $n = 0$  and  $n = 1$  the quantity  $\hat{n}^2 - \hat{n}$  is zero, as follows:

$$\begin{aligned} & -\lambda^2 (I - 4\hat{n} + 2\hat{n}^2) \sigma^z \\ &= -\lambda^2 (I - 2n) \sigma^z. \end{aligned} \quad (239)$$

The gate is therefore directly synthesized as the product of the qubit rotation gate  $\exp(-\lambda^2 \sigma^z)$  and the  $z$ -conditional rotation gate  $\exp(2\lambda^2 \hat{n} \sigma^z)$  for a lower bound gate depth of two.

## E.1 Effective Hubbard-lattice interaction approach

An alternative scheme to encode a qubit in a cavity with the instruction set is to map the three-dimensional quantum electrodynamics (3D cQED) system to a qubit by imposing an  $\hat{n}(\hat{n} - 1)$  anharmonicity into the Jaynes-Cummings Hamiltonian that describes the system. The anharmonicity term increases the energy gap between higher levels of the oscillator to effectively restrict propagation to the span  $\{|0\rangle, |1\rangle\}$  Fock space in which there is universal control.

Consider the standard Jaynes-Cummings Hamiltonian

$$\hat{H}_{\text{JC}} = \omega_R \hat{a}^\dagger \hat{a} + \frac{\omega_Q}{2} \sigma^z + g (\hat{a} \sigma^+ + \hat{a}^\dagger \sigma^-), \quad (240)$$

where  $\omega_R$  is the cavity frequency,  $\omega_Q$  is the qubit frequency, and  $g$  is the coupling parameter. Inclusion of the simulated  $\hat{n}(\hat{n} - 1)$  anharmonicity of strength  $\Gamma$  yields

$$\hat{H}_{\text{an}} = \omega_R \hat{a}^\dagger \hat{a} + \Gamma \hat{n}(\hat{n} - 1) + \frac{\omega_Q}{2} \sigma^z + g(\hat{a} \sigma^+ + \hat{a}^\dagger \sigma^-), \quad (241)$$

and the system is switched between states  $|0\rangle$  and  $|1\rangle$  with a weak time- $t$ -dependent drive of strength  $\Omega$  at the resonance frequency  $\omega_R$ , as follows:

$$\hat{H}_{\text{drive}}(t) = \Omega e^{i\omega_R t} \hat{a}^\dagger + \Omega^* e^{-i\omega_R t} \hat{a}. \quad (242)$$

Synthesis of a propagator of the form  $\exp(i\lambda^2 \hat{n}(\hat{n} - 1))$  is then sufficient to employ the native 3D cQED system as a qubit. Note the choice of  $\lambda$  for practical implementation must take into account both the time step and the fact the BCH decomposition yields a square root in the exponential argument. The required propagator is a Trotter-Suzuki decomposition of  $\exp\left(\left[\hat{A}, \hat{B}\right] \lambda^2\right) = \exp(i\lambda^2 \hat{n}^2 \sigma^z)$  and  $\exp(-i\lambda^2 \hat{n} \sigma^z)$ .

The first term is synthesized according to the BCH formula with a commutator determined by the Pauli commutation relation Eq. (16) as follows:

$$[\hat{A}, \hat{B}] = i\hat{n}^2\sigma^z \quad (243)$$

$$= i\hat{n}^2 \left( -\frac{i}{2} [\sigma^x, \sigma^y] \right) \quad (244)$$

$$= \left[ \frac{1}{\sqrt{2}}\hat{n}\sigma^x, \frac{1}{\sqrt{2}}\hat{n}\sigma^y \right], \quad (245)$$

where  $\hat{A}$  and  $\hat{B}$  correspond to  $x$ -conditional and  $y$ -conditional rotations, respectively. The second term is a  $z$ -conditional rotation gate.

The resulting anharmonicity gate therefore has a gate depth of lower bound five displacement and rotation gates or 45 displacement gates.

## F Fermi-Hubbard Lattice Dynamics

To further demonstrate the power of the ISA, we employ the approach to simulate fermionic dynamics on bosonic 3D cQED systems. We consider the Fermi-Hubbard lattice Hamiltonian

$$\hat{H}_{\text{FH}} = \hat{T}_{\text{FH}} + \hat{V}_{\text{FH}}, \quad (246)$$

$$\hat{T}_{\text{FH}} = -J \sum_{i,\sigma} \hat{c}_{i,\sigma}^\dagger \hat{c}_{i+1,\sigma} + \hat{c}_{i+1,\sigma}^\dagger \hat{c}_{i,\sigma}, \quad (247)$$

$$\hat{V}_{\text{FH}} = U \sum_i \hat{n}_{i,\uparrow} \hat{n}_{i,\downarrow}. \quad (248)$$

The kinetic energy term  $\hat{T}_{\text{FH}}$  describes the nearest-neighbor interaction for hopping of a single spin between two sites with hopping parameter  $J$  and spin  $\sigma$  given annihilation operators  $\{\hat{c}_{j,\sigma}\}$  and creation operators  $\{\hat{c}_{j,\sigma}^\dagger\}$  for sites  $\{j\}$ . The potential energy term  $\hat{V}_{\text{FH}}$  describes the same-site interaction, which gives the energetic unfavorability of a spin up  $\uparrow$  and spin down  $\downarrow$  coexisting on the same site  $i$ , where  $\hat{n}_{j,\sigma}$  gives the number of spin  $\sigma$  particles on site  $j$ . According to fermion statistics, no more than a single particle of a given spin can exist on a single site.

Each cavity of the 3D cQED system represents either a spin up or spin down particle on a single lattice site, for direct comparison to the qubit-based schemes of refs. [35, 36, 37]. Each cavity is connected to the cavity that represents the same site of opposite spin to facilitate computation of the potential energy  $\hat{V}_{\text{FH}}$ , as well as to cavities of the same spin on neighboring sites to facilitate computation of the kinetic energy  $\hat{T}_{\text{FH}}$ . Cavities are also connected along Jordan-Wigner strings to take into account fermionic statistics.

The  $|0\rangle$  cavity state represents absence of a spin and the  $|1\rangle$  state represents presence of a spin. Within each cavity, only the states in span  $\{|0\rangle, |1\rangle\}$  are considered, as in Section (E), which prevents leakage into unphysical high-energy cavity states. At the end of each operation, the cavity state must be in either the  $|0\rangle$  or  $|1\rangle$  state and the transmon state must also be in the ground state  $|g\rangle$ , which provides an error syndrome and therefore a degree of error detection not employed in qubit-based representations of the Fermi-Hubbard lattice.

Propagation of any combination of up spins and down spins is simulated with three two-cavity gates. The first two gates – the same-site and hopping gates – are defined as the propagator of the

same-site and hopping Hamiltonians, respectively. The same-site term of the Hamiltonian for site  $i$  is

$$\hat{H}_{\text{same}} = U \hat{n}_{i,\uparrow} \hat{n}_{i,\downarrow}. \quad (249)$$

This term is zero if only one spin is on a site and  $U$  if both spins are on the same site, which gives the diagonal Hamiltonian in the reduced  $4 \times 4$  Hilbert space

$$\hat{H}_{\text{same}} = \begin{bmatrix} 0 & 0 & 0 & 0 \\ 0 & 0 & 0 & 0 \\ 0 & 0 & 0 & 0 \\ 0 & 0 & 0 & U \end{bmatrix} \quad (250)$$

and the diagonal propagator  $U_{\text{same}} = e^{-i\hat{H}_{\text{same}}\tau}$

$$U_{\text{same}} = \begin{bmatrix} 1 & 0 & 0 & 0 \\ 0 & 1 & 0 & 0 \\ 0 & 0 & 1 & 0 \\ 0 & 0 & 0 & e^{-iU\tau} \end{bmatrix}. \quad (251)$$

This gate is recognized as the conditional cross-Kerr interaction of 3D cQED systems and equivalently a controlled-phase (CPHASE) gate in the reduced subspace span  $\{|0\rangle, |1\rangle\}$ . The hopping term of the Hamiltonian for each  $\sigma$  spin in sites  $i, (i+1)$  is

$$H_{\text{hop}} = -J \left( \hat{c}_{i,\sigma}^\dagger \hat{c}_{i+1,\sigma} + \hat{c}_{i+1,\sigma}^\dagger \hat{c}_{i,\sigma} \right) \quad (252)$$

$$= -J \left( \hat{c}_{i,\sigma}^\dagger \hat{c}_{i+1,\sigma} - \hat{c}_{i,\sigma} \hat{c}_{i+1,\sigma}^\dagger \right), \quad (253)$$

where the latter expression employs the commutator relationship of the annihilation and creation operators. The hopping Hamiltonian for the specified mapping is then the off-diagonal matrix

$$H_{\text{hop}} = \begin{bmatrix} 0 & 0 & 0 & 0 \\ 0 & 0 & -t & 0 \\ 0 & -t & 0 & 0 \\ 0 & 0 & 0 & 0 \end{bmatrix}, \quad (254)$$

which gives the hopping propagator  $U_{\text{hop}} = e^{-iH_{\text{hop}}\tau}$

$$U_{\text{hop}} = \begin{bmatrix} 1 & 0 & 0 & 0 \\ 0 & \cos(t\tau) & i \sin(t\tau) & 0 \\ 0 & i \sin(t\tau) & \cos(t\tau) & 0 \\ 0 & 0 & 0 & 1 \end{bmatrix}, \quad (255)$$

which is recognized as a conditional controlled-phase beam splitter restricted to span  $\{|0\rangle, |1\rangle\}$  in bosonic systems and a Givens or iSWAP-like gate in the reduced span  $\{|0\rangle, |1\rangle\}$  subspace [37, 36]. The final gate of the three-gate set incorporates the fermionic statistics of the spins via the fermionic SWAP (FSWAP) gate [35, 37]. The content of each cavity is swapped with one of its neighbors with inclusion of a phase where both spins are present in neighboring cavities as follows

$$U_{\text{FSWAP}} = \begin{bmatrix} 1 & 0 & 0 & 0 \\ 0 & 0 & 1 & 0 \\ 0 & 1 & 0 & 0 \\ 0 & 0 & 0 & -1 \end{bmatrix}, \quad (256)$$

which is recognized as the product of a conditional rotation gate and a beam-splitter on 3D cQED systems.

Finally, initial states are prepared by the universal set of gates in span  $\{|0\rangle, |1\rangle\}$  detailed in Section E.

### F.1 Conditional cross-Kerr (CPHASE) gate

We consider the infinitesimal conditional cross-Kerr gate

$$U_{\text{cross-Kerr}} = e^{i\lambda^2 \hat{n}_1 \hat{n}_2 \sigma_z}, \quad (257)$$

which is also employed in GKP codes encoded in 3D cQED systems [38].

The argument is expressed in terms of a commutator according to the Pauli commutation relation Eq. 16, as follows:

$$[A, B]\lambda^2 = i\lambda^2 \hat{n}_1 \hat{n}_2 \sigma_z \quad (258)$$

$$= i\lambda^2 \hat{n}_1 \hat{n}_2 \left( -\frac{i}{2} [\sigma^x, \sigma^y] \right) \quad (259)$$

$$= \left[ \frac{1}{\sqrt{2}} \hat{n}_1 \sigma^x, \frac{1}{\sqrt{2}} \hat{n}_2 \sigma^y \right] \lambda^2, \quad (260)$$

where  $\hat{A}$  corresponds to an  $x$ -conditional rotation gate and  $B$  corresponds to a  $y$ -conditional rotation gate.

The resulting gate features a lower bound gate depth of four displacement and rotation gates or 16 displacement gates.

### F.2 Span $\{|0\rangle, |1\rangle\}$ conditional beam splitter gate

In order to generate a span  $\{|0\rangle, |1\rangle\}$  that operates only when  $\hat{n}_1 \hat{n}_2 \neq 1$  (*i.e.*,  $1 - \hat{n}_1 \hat{n}_2 = 0$ ), we formulate the infinitesimal conditional (controlled-phase) beam-splitter gate

$$U_{\text{cond. beam}} = e^{-i\lambda^2 (\hat{a}_1^\dagger \hat{a}_2 + \hat{a}_1 \hat{a}_2^\dagger) (1 - \hat{n}_1 \hat{n}_2) \sigma^z}, \quad (261)$$

which is decomposed via the Trotter-Suzuki decomposition in terms of  $\exp\left(-i\lambda^2 (\hat{a}_1^\dagger \hat{a}_2 + \hat{a}_1 \hat{a}_2^\dagger) \sigma^z\right)$  and  $\exp\left(i\lambda^2 (\hat{a}_1^\dagger \hat{a}_2 + \hat{a}_1 \hat{a}_2^\dagger) (\hat{n}_1 \hat{n}_2) \sigma^z\right)$ . The first term is the conditional beam splitter  $U_{\text{beam split}}$  Eq. 4.4 and the second term is decomposed via BCH as follows:

Given the expression of the number operator in terms of the phase-space operators Eq. 55, the argument of the second exponential operator is

$$\begin{aligned} & i\lambda^2 (\hat{a}_1^\dagger \hat{a}_2 + \hat{a}_1 \hat{a}_2^\dagger) \hat{n}_1 \hat{n}_2 \sigma^z \\ &= i\lambda^2 (2(\hat{x}_1 \hat{x}_2 + \hat{p}_1 \hat{p}_2)) \hat{n}_1 \hat{n}_2 \sigma^z. \end{aligned} \quad (262)$$

The term is then expressed as a Trotter decomposition of  $\exp\left(\left[\hat{A}_1, \hat{B}_1\right] \lambda^2\right) = \exp(2i\lambda^2 \hat{x}_1 \hat{x}_2 \hat{n}_1 \hat{n}_2 \sigma^z)$  and  $\exp\left(\left[\hat{A}_2, \hat{B}_2\right] \lambda^2\right) = \exp(2i\lambda^2 \hat{p}_1 \hat{p}_2 \hat{n}_1 \hat{n}_2 \sigma^z)$ .

The first commutator is given by the Pauli commutation relation Eq. 16

$$[\hat{A}_1, \hat{B}_1] = 2i\hat{x}_1\hat{x}_2\hat{n}_1\hat{n}_2\sigma^z \quad (263)$$

$$= 2i\hat{x}_1\hat{x}_2\hat{n}_1\hat{n}_2 \left( -\frac{i}{2} [\sigma^x, \sigma^y] \right) \quad (264)$$

$$= [\hat{x}_1\hat{n}_1\sigma^x, \hat{x}_2\hat{n}_2\sigma^y]. \quad (265)$$

The  $\hat{A}_1$  term is determined by a Trotter decomposition such that

$$\hat{A}_1 = \frac{1}{2} \{\hat{x}_1, \hat{n}_1\} \sigma^x + \frac{1}{2} [\hat{x}_1, \hat{n}_1] \sigma^x \quad (266)$$

$$= \hat{A}_{1a} + \hat{A}_{1b}, \quad (267)$$

where according to the anticommutator to commutator relation  $\hat{A}_{1a}$  is given by the BCH formula with

$$[\hat{A}_{1a'}, \hat{B}_{1a'}] = \frac{1}{2} \{\hat{x}_1, \hat{n}_1\} \sigma^x \quad (268)$$

$$= \frac{i}{2} [i\hat{x}_1\sigma^y, i\hat{n}_1\sigma^z] \quad (269)$$

$$= \left[ -\frac{1}{\sqrt{2}}\hat{x}_1\sigma^y, -\frac{1}{\sqrt{2}}\hat{n}_1\sigma^z \right], \quad (270)$$

where  $\hat{B}_{1a'}$  is a  $z$ -conditional rotation gate. Distribution of terms yields  $\hat{A}_{1b}$  as

$$[\hat{A}_{1b'}, \hat{B}_{1b'}] = \left[ \frac{1}{\sqrt{2}}\hat{x}_1, \frac{1}{\sqrt{2}}\hat{n}_1\sigma^x \right], \quad (271)$$

where  $B_{1b'}$  is an  $x$ -conditional rotation gate.

According to the same procedure,

$$\hat{B}_1 = \frac{1}{2} \{\hat{x}_2, \hat{n}_2\} \sigma^y + \frac{1}{2} [\hat{x}_2, \hat{n}_2] \sigma^y \quad (272)$$

$$= \hat{B}_{1a} + \hat{B}_{1b}, \quad (273)$$

where  $\hat{B}_{1a}$  is given by

$$[\hat{A}_{1a''}, \hat{B}_{1a''}] = \frac{1}{2} \{\hat{x}_2, \hat{n}_2\} \sigma^y \quad (274)$$

$$= \frac{i}{2} [i\hat{x}_2\sigma^z, i\hat{n}_1\sigma^x] \quad (275)$$

$$= \left[ -\frac{1}{\sqrt{2}}\hat{x}_2\sigma^z, -\frac{1}{\sqrt{2}}\hat{n}_2\sigma^x \right], \quad (276)$$

with  $B_{1a''}$  an  $x$ -conditional rotation, and  $B_{1b}$  is given by

$$[\hat{A}_{1b''}, \hat{B}_{1b''}] = \left[ \frac{1}{\sqrt{2}}\hat{x}_2, \frac{1}{\sqrt{2}}\hat{n}_2\sigma^y \right], \quad (277)$$

where  $B_{1b''}$  is a  $y$ -conditional rotation gate. The second term follows analogously with the position  $x$  replaced by the momentum  $p$ .

### F.3 Conditional FSWAP gate

The FSWAP gate follows immediately from the conditional cross-Kerr gate detailed above and a complete beam-splitter gate (or conditional beam-splitter gate detailed above) as

$$U_{\text{FSWAP}} = U_{\text{cond. Kerr}} U_{\text{cond. beam}}. \quad (278)$$

## References

- [1] F. Arute, K. Arya, R. Babbush, D. Bacon, J. C. Bardin, R. Barends, R. Biswas, S. Boixo, F. G. Brandao, D. A. Buell, et al. Quantum supremacy using a programmable superconducting processor. *Nature*, 574(7779):505–510, 2019.
- [2] O. Dial. Moving the needle on scale. In *American Physical Society (March Meeting)*, 2022.
- [3] M. Reagor, C. B. Osborn, N. Tezak, A. Staley, G. Prawiroatmodjo, M. Scheer, N. Alidoust, E. A. Sete, N. Didier, M. P. da Silva, et al. Demonstration of universal parametric entangling gates on a multi-qubit lattice. *Sci. Adv.*, 4(2):eaao3603, 2018.
- [4] K. Wright, K. M. Beck, S. Debnath, J. Amini, Y. Nam, N. Grzesiak, J.-S. Chen, N. Pimenti, M. Chmielewski, C. Collins, et al. Benchmarking an 11-qubit quantum computer. *Nat. Commun.*, 10(1):1–6, 2019.
- [5] C. S. Wang, J. C. Curtis, B. J. Lester, Y. Zhang, Y. Y. Gao, J. Freeze, V. S. Batista, P. H. Vaccaro, I. L. Chuang, L. Frunzio, L. Jiang, S. M. Girvin, and R. J. Schoelkopf. Efficient multiphoton sampling of molecular vibronic spectra on a superconducting bosonic processor. *Phys. Rev. X*, 10:021060, 2, 2020.
- [6] C. S. Wang, N. E. Frattini, B. J. Chapman, S. Puri, S. M. Girvin, M. H. Devoret, and R. J. Schoelkopf. Observation of wave-packet branching through an engineered conical intersection. *arXiv:2202.02364*, 2022.
- [7] A. Petrescu, H. E. Türeci, A. V. Ustinov, and I. M. Pop. Fluxon-based quantum simulation in circuit QED. *Phys. Rev. B*, 98:174505, 17, 2018.
- [8] A. Blais, A. L. Grimsmo, S. M. Girvin, and A. Wallraff. Circuit quantum electrodynamics. *Rev. Mod. Phys.*, 93(2):025005, 2021.
- [9] A. Sørensen and K. Mølmer. Quantum computation with ions in thermal motion. *Phys. Rev. Lett.*, 82:1971–1974, 9, March 1999.
- [10] N. Lauk, N. Sinclair, S. Barzanjeh, J. P. Covey, M. Saffman, M. Spiropulu, and C. Simon. Perspectives on quantum transduction. *Quantum Sci. Technol.*, 5(2):020501, 2020.
- [11] D. Basilewitsch, Y. Zhang, S. M. Girvin, and C. P. Koch. Engineering strong beamsplitter interaction between bosonic modes via quantum optimal control theory. *Phys. Rev. Res.*, 4(2):023054, 2022.
- [12] T. J. Stavenger, E. Crane, K. Smith, C. T. Kang, S. M. Girvin, and N. Wiebe. Bosonic Qiskit. *2022 IEEE High Performance Extreme Computing Conference (HPEC)*, eCF Paper Id: HPEC2022-52 (<https://doi.org/10.48550/arXiv.2209.11153>), 2022.
- [13] N. Khaneja, T. Reiss, C. Kehlet, T. Schulte-Herbrüggen, and S. J. Glaser. Optimal control of coupled spin dynamics: design of NMR pulse sequences by gradient ascent algorithms. *J. Magn. Reson.*, 172(2):296–305, 2005.

- [14] J. Werschnik and E. Gross. Quantum optimal control theory. *J. Phys. B: At. Mol. Opt. Phys.*, 40(18):R175, 2007.
- [15] M. H. Goerz, F. Motzoi, K. B. Whaley, and C. P. Koch. Charting the circuit QED design landscape using optimal control theory. *npj Quantum Inf.*, 3(1):37, 2017. ISSN: 2056-6387.
- [16] R. W. Heeres, B. Vlastakis, E. Holland, S. Krastanov, V. V. Albert, L. Frunzio, L. Jiang, and R. J. Schoelkopf. Cavity state manipulation using photon-number selective phase gates. *Phys. Rev. Lett.*, 115:137002, 13, September 2015.
- [17] A. Eickbusch, V. Sivak, A. Z. Ding, S. S. Elder, S. R. Jha, J. Venkatraman, B. Royer, S. M. Girvin, R. J. Schoelkopf, and M. H. Devoret. Fast universal control of an oscillator with weak dispersive coupling to a qubit. *Nat. Phys.*, 18(12):1464–1469, 2022. ISSN: 1745-2481.
- [18] M. Pechal, L. Huthmacher, C. Eichler, S. Zeytinoglu, A. A. Abdumalikov, S. Berger, A. Wallraff, and S. Filipp. Microwave-controlled generation of shaped single photons in circuit quantum electrodynamics. *Phys. Rev. X*, 4:041010, 4, October 2014.
- [19] S. Zeytinoglu, M. Pechal, S. Berger, A. A. Abdumalikov, A. Wallraff, and S. Filipp. Microwave-induced amplitude- and phase-tunable qubit-resonator coupling in circuit quantum electrodynamics. *Phys. Rev. A*, 91:043846, 4, April 2015.
- [20] S. Rosenblum, Y. Y. Gao, P. Reinhold, C. Wang, C. J. Axline, L. Frunzio, S. M. Girvin, L. Jiang, M. Mirrahimi, M. H. Devoret, and R. J. Schoelkopf. A CNOT gate between multiphoton qubits encoded in two cavities. *Nature Commun.*, 9(1):652, 2018. ISSN: 2041-1723.
- [21] O. Milul, B. Guttel, U. Goldblatt, S. Hazanov, L. M. Joshi, D. Chausovsky, N. Kahn, E. Çiftyürek, F. Lafont, and S. Rosenblum. A superconducting quantum memory with tens of milliseconds coherence time, 2023.
- [22] A. M. Childs, Y. Su, M. C. Tran, N. Wiebe, and S. Zhu. Theory of Trotter error with commutator scaling. *Phys. Rev. X*, 11(1):011020, 2021.
- [23] D. W. Berry, G. Ahokas, R. Cleve, and B. C. Sanders. Efficient quantum algorithms for simulating sparse Hamiltonians. *Commun. Math. Phys.*, 270:359–371, 2007.
- [24] Y. Su, D. W. Berry, N. Wiebe, N. Rubin, and R. Babbush. Fault-tolerant quantum simulations of chemistry in first quantization. *PRX Quantum*, 2(4):040332, 2021.
- [25] A. M. Childs and N. Wiebe. Product formulas for exponentials of commutators. *J. Math. Phys.*, 54(6):062202, 2013. ISSN: 1089-7658.
- [26] J. M. Martyn, Z. M. Rossi, A. K. Tan, and I. L. Chuang. Grand unification of quantum algorithms. *PRX Quantum*, 2(4):040203, 2021.
- [27] Q. Zhao, Y. Zhou, A. F. Shaw, T. Li, and A. M. Childs. Hamiltonian simulation with random inputs. *arXiv preprint arXiv:2111.04773*, 2021.
- [28] C. S. Wang, J. C. Curtis, B. J. Lester, Y. Zhang, Y. Y. Gao, J. Freeze, V. S. Batista, P. H. Vaccaro, I. L. Chuang, L. Frunzio, L. Jiang, S. M. Girvin, and R. J. Schoelkopf. Efficient multiphoton sampling of molecular vibronic spectra on a superconducting bosonic processor. *Phys. Rev. X*, 10:021060, 2, June 2020.
- [29] J. C. Curtis, C. T. Hann, S. S. Elder, C. S. Wang, L. Frunzio, L. Jiang, and R. J. Schoelkopf. Single-shot number-resolved detection of microwave photons with error mitigation. *Phys. Rev. A*, 103:023705, 2, February 2021.

- [30] Y. Y. Gao, B. J. Lester, K. S. Chou, L. Frunzio, M. H. Devoret, L. Jiang, S. Girvin, and R. J. Schoelkopf. Entanglement of bosonic modes through an engineered exchange interaction. *Nature*, 566(7745):509–512, 2019.
- [31] I. Pietikäinen, O. Černotík, S. Puri, R. Filip, and S. M. Girvin. Controlled beam splitter gate transparent to dominant ancilla errors. *Quantum Sci. Technol.*, 2022.
- [32] T. Fösel, S. Krastanov, F. Marquardt, and L. Jiang. Efficient cavity control with SNAP gates. *arXiv preprint arXiv:2004.14256*, 2020.
- [33] M. A. Nielsen and I. L. Chuang. *Quantum Computation and Quantum Information: 10th Anniversary Edition*. Cambridge University Press, 2010.
- [34] Y. Liu, J. Sinanan-Singh, M. T. Kearney, G. Mintzer, and I. L. Chuang. Constructing qudits from infinite-dimensional oscillators by coupling to qubits. *Phys. Rev. A*, 104(3):032605, 2021.
- [35] I. D. Kivlichan, J. McClean, N. Wiebe, C. Gidney, A. Aspuru-Guzik, G. K.-L. Chan, and R. Babbush. Quantum simulation of electronic structure with linear depth and connectivity. *Phys. Rev. Lett.*, 120(11):110501, March 2018.
- [36] F. Arute, K. Arya, R. Babbush, D. Bacon, J. C. Bardin, R. Barends, A. Bengtsson, S. Boixo, M. Broughton, B. B. Buckley, et al. Observation of separated dynamics of charge and spin in the Fermi-Hubbard model. *arXiv preprint arXiv:2010.07965*, 2020.
- [37] C. Cade, L. Mineh, A. Montanaro, and S. Stanisic. Strategies for solving the Fermi-Hubbard model on near-term quantum computers. *Phys. Rev. B*, 102(23):235122, December 2020.
- [38] B. Royer, S. Singh, and S. Girvin. Encoding qubits in multimode grid states. *PRX Quantum*, 3(1):010335, 2022.